

FOURIER TRANSFORM OF RAUZY FRACTALS AND POINT SPECTRUM OF 1D PISOT INFLATION TILINGS

MICHAEL BAAKE AND UWE GRIMM

ABSTRACT. Primitive inflation tilings of the real line with finitely many tiles of natural length and a Pisot–Vijayaraghavan unit as inflation factor are considered. We present an approach to the pure point part of their diffraction spectrum on the basis of a Fourier matrix cocycle in internal space. This cocycle leads to a transfer matrix equation and thus to a closed expression of matrix Riesz product type for the Fourier transforms of the windows for the covering model sets. In general, these windows are complicated Rauzy fractals and thus difficult to handle. Equivalently, this approach permits a construction of the (always continuous) eigenfunctions for the translation dynamical system induced by the inflation rule. We review and further develop the underlying theory, and apply it to the family of Pisa substitutions, with special emphasis on the Tribonacci case.

1. INTRODUCTION

Inflation tilings of the of line with an inflation (or stretching) factor λ that is a Pisot–Vijayaraghavan (PV) number are intimately related to cut and project sets. In the best case, which is the topic of the famous Pisot substitution conjecture [45, 1], their vertex points (in the geometric realisation with intervals of natural length) are regular model sets themselves, and thus have pure point spectrum, equivalently in the dynamical or in the diffraction sense [29, 8, 9]. More generally, they might have mixed spectrum, see [4, 5] and references therein for examples, but the PV-nature of λ still implies that they lead to Meyer sets and thus have non-trivial point spectrum [50, Sec. 5.10]; see also [49].

When analysing such inflation tilings, one quickly encounters covering model sets with complicated windows, known as Rauzy fractals [41, 39], which are compact sets of positive measure that are topologically regular (that is, they are the closure of their interior) and perfect (that is, they have no isolated points), but display a fractal boundary and often also a non-trivial fundamental group. While a lot is known about Rauzy fractals, see [44, 45, 39] and references therein, it is not obvious how to calculate their Fourier transform in closed form, which is needed to determine the diffraction intensities of the tiling system explicitly. Phrased differently, but equivalently, this Fourier transform is also needed to calculate the eigenfunctions of the corresponding dynamical system under the translation action of \mathbb{R} ; compare [30, 9].

The purpose of this contribution is to reconsider this problem in a constructive and computational way. In particular, our goal is to make the Fourier–Bohr coefficients or amplitudes (and thus also the eigenfunctions) of such inflation tilings available, via a quadratic form with

a matrix that can be written as an infinite matrix Riesz product. Since the latter turns out to be compactly and rapidly converging, all quantities are efficiently computable. Here, we solve the problem for inflation tilings of the real line with finitely many prototiles and an inflation factor that is a PV unit. The extension to general PV numbers and to higher dimensions will be treated separately, as this requires a bigger machinery, algebraically and analytically.

The paper is organised as follows. We begin by recalling the setting of inflation tilings of the real line in Section 2. Then, in Section 3, we introduce the Minkowski embedding and the description of our tilings (and point sets) in internal space, which leads to a contractive iterated function system for the windows of the covering model sets. This is followed by the introduction and analysis of an internal cocycle in Section 4, which leads to a matrix Riesz product expression for the Fourier transform of the Rauzy windows, and thus also for the spectral quantities we are after. In this context, in Section 5, we establish an important connection between the Fourier–Bohr coefficients of PV inflation point sets and those of the covering model sets, which emerges through a specific uniform distribution result. Then, in Section 6, we embark on a number of illustrative examples from the family of Pisa substitutions (including some based on cubic and quartic number fields), followed by an example of covering degree 2 in Section 7 and a brief outlook.

2. INFLATION TILINGS OF THE REAL LINE

Let us begin with the symbolic side of the problem, where we consider a primitive substitution ϱ on a finite alphabet $\mathcal{A} = \{a_1, \dots, a_N\}$. Here, the mapping $a_i \mapsto \varrho(a_j)$ is usually specified by the N -tuple $(\varrho(a_1), \dots, \varrho(a_N))$. The *substitution matrix* of ϱ is M , where M_{ij} counts the number of letters of type a_i in $\varrho(a_j)$; see [39, 40, 6] for general background and results. We denote the characteristic polynomial of M by $p(x)$, which is monic, but need not be irreducible over \mathbb{Z} in our setting, meaning that we can also include a variety of systems with mixed spectrum.

Let $\lambda = \lambda_{\text{PF}}$ be the Perron–Frobenius (PF) eigenvalue of M . As M is primitive by assumption, we know that there are strictly positive left and right eigenvectors for λ , denoted¹ by $\langle u|$ and $|v\rangle$, which we assume to be normalised such that

$$\langle 1|v\rangle = \langle u|v\rangle = 1.$$

Here, $\langle 1| := \langle 1, \dots, 1|$ is the row vector with N equal entries 1. In the substitution context, the first condition thus ensures that the entries of $|v\rangle$ encode the relative letter frequencies in the symbolic sequences defined by ϱ , while the second condition implies that

$$(1) \quad P := |v\rangle\langle u|$$

¹Since we will be using left and right eigenvectors throughout, we adopt Dirac’s bra-c-ket notation, where $\langle u|v\rangle$ then stands for the sesquilinear inner product in \mathbb{C}^N , which becomes bilinear when restricted to \mathbb{R}^N .

is a projector of rank 1, so $P^2 = P$ with $P(\mathbb{R}^N) = \text{im}(P) = \mathbb{R}|v\rangle$, where all entries of $P \in \text{Mat}(N, \mathbb{R})$ are strictly positive. Now, let $\|\cdot\|$ be any matrix norm, not necessarily a sub-multiplicative one. Then, the following property is standard; see [22, Thm. 8.5.1].

Fact 2.1. *For a primitive, non-negative matrix $M \in \text{Mat}(N, \mathbb{R})$ with PF eigenvalue λ , one has $\lim_{n \rightarrow \infty} \lambda^{-n} M^n = P$, with the projector P from (1). This convergence also entails that $0 < \sup_{n \in \mathbb{N}} \|\lambda^{-n} M^n\| < \infty$. \square*

Working with PV substitutions, we may as well profit from the underlying geometry by turning the symbolic sequences into tilings; see [48, 6] for general background and [14, 15] for the justification why this does not change the spectral type of our system. Here, we choose intervals of natural length, meaning proportional to the entries of $\langle u|$, with control points on their left endpoints. As all entries u_i of $\langle u|$ lie in $\mathbb{Q}(\lambda)$, one normally multiplies them with their common denominator, so that they become elements of $\mathbb{Z}[\lambda]$. For each sequence in the symbolic hull defined by ϱ , this leads to a multi-component or *typed* point set, $\Lambda = \bigcup_i \Lambda_i$, where the Λ_i emerge from the N distinct types of control points and now form pairwise disjoint subsets of $\mathbb{Z}[\lambda]$.

Remark 2.2. Let us mention one consequence of the geometric setting. When $\ell_i = \alpha u_i$ with $1 \leq i \leq N$ are the chosen interval lengths, the average distance between neighbouring control points in Λ is well defined, compare [6, Sec. 4.3], and reads

$$\bar{\ell} = \sum_{i=1}^N v_i \ell_i = \alpha \langle u|v \rangle = \alpha,$$

so we get $\text{dens}(\Lambda) = 1/\alpha$ as the density of Λ , and $\text{dens}(\Lambda_i) = v_i \text{dens}(\Lambda)$ for $1 \leq i \leq N$. \diamond

Next, we define the set-valued *displacement matrix* $T = (T_{ij})_{1 \leq i, j \leq N}$, where the set T_{ij} consists of all relative (geometric) positions of tiles of type a_i in the supertile² $\varrho(a_j)$; see [3, 4, 5] for background. This gives rise to the *Fourier matrix* of ϱ via $B := \widetilde{\delta}_T$, so

$$B_{ij}(k) = \sum_{x \in T_{ij}} e^{2\pi i x k}, \quad k \in \mathbb{R},$$

which is a trigonometric polynomial. Since $\text{card}(T_{ij}) = M_{ij}$, one has the inequality

$$(2) \quad |B_{ij}(k)| \leq M_{ij}$$

for all i, j and all $k \in \mathbb{R}$, where we get equality for $k = 0$ because $B(0) = M$.

Given B , we construct a *cocycle* (in the sense of [12, Sec. 2.1], over the dilation $k \mapsto \lambda k$) from the Fourier matrix, via

$$(3) \quad B^{(n)}(k) := B(k)B(\lambda k) \cdots B(\lambda^{n-1}k),$$

²Note that, by slight abuse of notation, we use ϱ both for the symbolic substitution and for the geometric inflation, where the meaning will always be clear from the context.

so $B^{(1)}(k) = B(k)$ together with

$$(4) \quad B^{(n+1)}(k) = B^{(n)}(k)B(\lambda^n k) = B(k)B^{(n)}(\lambda k)$$

for $n \geq 1$. Inductively, one can check that $B^{(n)}(k)$ is the Fourier matrix of ϱ^n , see [5, Fact 3.6], with $B^{(n)}(0) = M^n$.

Recall that a matrix norm $\|\cdot\|$ is called *weakly monotone* when $\|A\| \leq \||A|\|$ holds for all $A \in \text{Mat}(N, \mathbb{C})$, where $|A|$ denotes the matrix with entries $|A_{ij}|$; see [26] for a general exposition of monotonicity properties of vector and matrix norms. With this and Eq. (2), the following property is immediate from Fact 2.1.

Fact 2.3. *The entries of the cocycle (4) satisfy $|B_{ij}^{(n)}(k)| \leq (M^n)_{ij}$, for all i, j and all $k \in \mathbb{R}$. Consequently, if $\|\cdot\|$ is any weakly monotone matrix norm, $\|\lambda^{-n}B^{(n)}(k)\|$ is uniformly bounded on \mathbb{R} , which means that*

$$c_B := \sup_{n \in \mathbb{N}} \sup_{k \in \mathbb{R}} \|\lambda^{-n}B^{(n)}(k)\|$$

is finite, with $0 < c_B < \infty$. Moreover, for all i, j and all $k \in \mathbb{R}$, one has

$$0 \leq \liminf_{n \rightarrow \infty} \lambda^{-n}|B_{ij}^{(n)}(k)| \leq \limsup_{n \rightarrow \infty} \lambda^{-n}|B_{ij}^{(n)}(k)| \leq P_{ij},$$

where the P_{ij} are the matrix elements of the projector P from Eq. (1). This leads to more specific results on c_B depending on the matrix norm chosen. \square

Let us from now on assume that λ is a PV unit of degree $d \leq N$. Since M is an integer matrix and the equations for the left and right eigenvector to λ can thus be solved in the field $\mathbb{Q}(\lambda)$, a natural object to consider is the \mathbb{Z} -module $L := \mathbb{Z}[\lambda] = \langle 1, \lambda, \dots, \lambda^{d-1} \rangle_{\mathbb{Z}}$ of rank d . This is the main reason to choose the interval lengths (ℓ_1, \dots, ℓ_N) for the tiling such that $\mathbb{Z}[\lambda]$ comprises all possible coordinates of our control points (relative to one of them, which may be placed at 0 without loss of generality). We assume that L is optimal relative to the control point set in the sense that no proper submodule of L comprises all of those points (otherwise, we change the natural interval lengths so that this is true). Next, we extract and harvest some intrinsic geometric information from this setting.

3. MINKOWSKI EMBEDDING AND INTERNAL SPACE

Let us recall the Minkowski embedding from [6, Sec. 3.4], now tailored to $L = \mathbb{Z}[\lambda]$. Since λ has degree d , this will lead to a lattice \mathcal{L} in \mathbb{R}^d as follows. There are r real algebraic conjugates of λ , and s complex conjugate pairs, so $d = r + 2s$, which are defined via the irreducible, monic polynomial in $\mathbb{Z}[x]$ that has λ as a root. This polynomial is a factor of the characteristic polynomial p of M in our case. Consequently, there are $r \geq 1$ real field isomorphisms $\kappa_1, \dots, \kappa_r$, with $\kappa_1 = \text{id}$, and $s \geq 0$ complex field isomorphisms $\sigma_1, \dots, \sigma_s$, together with their complex conjugates, $\bar{\sigma}_1, \dots, \bar{\sigma}_s$. In this setting, we can define a \mathbb{Z} -linear mapping $\Phi: \mathbb{Z}[\lambda] \rightarrow \mathbb{R}^d$ by

$$x \mapsto (x, \kappa_2(x), \dots, \kappa_r(x), \text{Re}(\sigma_1(x)), \text{Im}(\sigma_1(x)), \dots, \text{Re}(\sigma_s(x)), \text{Im}(\sigma_s(x))),$$

which extends to an \mathbb{Q} -linear mapping on the field $\mathbb{Q}(\lambda)$. Clearly, each image point is of the form $\Phi(x) = (x, x^*)$ with $x^* \in \mathbb{R}^{d-1}$. The induced map $\star: \mathbb{Q}(\lambda) \rightarrow \mathbb{R}^{d-1}$ is called the \star -map of the underlying cut and project scheme; compare [6, Sec. 7.2] or [35].

It is a standard result of algebraic number theory [36, Sec. I.5] that $\mathcal{L} := \Phi(L) = \Phi(\mathbb{Z}[\lambda])$ is indeed a lattice in \mathbb{R}^d , where we prefer the real version over the (algebraically) perhaps more natural one with $\mathbb{R}^r \times \mathbb{C}^s$ because we will need Fourier transforms shortly. So, we obtain the following Euclidean *cut and project scheme*, or CPS for short; see [6, Sec. 7.2] and references therein for more.

$$(5) \quad \begin{array}{ccccc} \mathbb{R} & \xleftarrow{\pi} & \mathbb{R} \times \mathbb{R}^{d-1} & \xrightarrow{\pi_{\text{int}}} & \mathbb{R}^{d-1} \\ \cup & & \cup & & \cup \text{ dense} \\ \pi(\mathcal{L}) & \xleftarrow{1-1} & \mathcal{L} & \longrightarrow & \pi_{\text{int}}(\mathcal{L}) \\ \parallel & & & & \parallel \\ L & \xrightarrow{\quad \star \quad} & & & L^* \end{array}$$

Here, π and π_{int} denote the canonical projections. Such a CPS is abbreviated as $(\mathbb{R}, \mathbb{R}^{d-1}, \mathcal{L})$.

To continue, observing that $\mathbb{R}^d = \mathbb{R} \times \mathbb{R}^{d-1}$, we also need the linear mapping Q on \mathbb{R}^{d-1} that is induced by the dilation $x \mapsto \lambda x$ (acting on the first component) in internal space. It is immediate from the structure of Φ and the CPS (5) that we get

$$(6) \quad Q = \text{diag}(\kappa_2(\lambda), \dots, \kappa_r(\lambda)) \oplus \bigoplus_{i=1}^s \begin{pmatrix} \text{Re}(\sigma_i(\lambda)) & -\text{Im}(\sigma_i(\lambda)) \\ \text{Im}(\sigma_i(\lambda)) & \text{Re}(\sigma_i(\lambda)) \end{pmatrix}.$$

Clearly, $Q \in \text{Mat}(d-1, \mathbb{R})$ is a normal matrix (so, $[Q^T, Q] = 0$) and a contraction, the latter because λ is a PV number, so all its algebraic conjugates lie strictly inside the unit disc.

Since $\{1, \lambda, \dots, \lambda^{d-1}\}$ is a \mathbb{Z} -basis of $\mathbb{Z}[\lambda]$, a basis matrix \mathcal{B} for \mathcal{L} can be chosen from here, with columns $\Phi(\lambda^i)^T$ for $0 \leq i \leq d-1$. The dual matrix, $\mathcal{B}^* := (\mathcal{B}^{-1})^T$, is then a basis matrix of the dual lattice,

$$\mathcal{L}^* := \{y \in \mathbb{R}^d : \langle x|y \rangle \in \mathbb{Z} \text{ for all } x \in \mathcal{L}\}.$$

Clearly, $\text{dens}(\mathcal{L}^*) = \text{dens}(\mathcal{L})^{-1} = |\det(\mathcal{B})|$.

Remark 3.1. The *Fourier module* of the underlying point set or tiling can be extracted from the first line of the dual basis matrix \mathcal{B}^* as

$$L^\circledast = \langle \mathcal{B}_{1i}^* : 1 \leq i \leq d \rangle_{\mathbb{Z}},$$

which is the projection of \mathcal{L}^* to the first component.

There is an intrinsic way to define L^\circledast as follows. With the Galois isomorphisms κ_i and σ_j from above, one defines the number-theoretic *trace* on $\mathbb{Q}(\lambda)$ as

$$(7) \quad \text{tr}(x) := \sum_{i=1}^r \kappa_i(x) + \sum_{j=1}^s (\sigma_j(x) + \bar{\sigma}_j(x)) = \sum_{i=1}^r \kappa_i(x) + 2 \sum_{j=1}^s \text{Re}(\sigma_j(x)).$$

Then, one has $L^\circledast = \{y \in \mathbb{Q}(\lambda) : \text{tr}(xy) \in \mathbb{Z} \text{ for all } x \in L\}$, which bypasses the explicit embedding step employed above, though it is of course equivalent to it.

In our setting, the Abelian group L^{\otimes} is the pure point part of the dynamical spectrum, in additive notation, for the tiling dynamical system induced by the inflation rule, where the dynamics is given by the translation action of \mathbb{R} ; see [9] for background. \diamond

To continue, in the spirit of [28], see also [6, Ch. 4], we return to the displacement matrix T of ϱ . By definition, when considering the a_i as tiles with natural length ℓ_i and left endpoint in 0, one has the stone inflation

$$\lambda a_i = \bigcup_{1 \leq j \leq N} \bigcup_{t \in T_{ji}} t + a_j.$$

More importantly, T enters the induced inflation action on the point sets via the iteration

$$(8) \quad A'_i = \dot{\bigcup}_{1 \leq j \leq N} \lambda A_j + T_{ij},$$

with a suitable and admissible initial condition, such as the left endpoints of a legal pair of intervals, one placed at 0 and the other at the fitting position to the left. The iteration then produces the control point sets of the corresponding successive tile inflations. The dot indicates that the union on the right-hand side of (8) is disjoint, while $+$ stands for the Minkowski sum of point sets; compare [6, Sec. 2.1].

Remark 3.2. Note that the iteration based on (8), viewed in the local topology, need not converge to a single typed point set $\Lambda = \bigcup_i A_i$. However, via a simple application of Dirichlet's pigeon hole principle, one can show that one converges to a finite cycle of such typed point sets, starting from a fixed, admissible (or legal) initial configuration. Each member of this cycle is equally well suited to define the (geometric) hull as an orbit closure under translations; compare [6, Chs. 4 and 5] for details. \diamond

Under the \star -map, (8) turns into an iteration of N finite (and hence closed) point sets in \mathbb{R}^{d-1} , and thus into an *iterated function system* (IFS) on $(\mathcal{K}\mathbb{R}^{d-1})^N$, where $\mathcal{K}\mathbb{R}^m$ with $m \in \mathbb{N}$ denotes the space of non-empty, compact subsets of \mathbb{R}^m , equipped with the Hausdorff (metric) topology; see [10] or [45, Sec. 4.6] and references therein for background. Here, the multiplication by λ is replaced by the action of the contraction Q from (6), giving

$$(9) \quad W_i = \bigcup_{1 \leq j \leq N} QW_j + T_{ij}^* = \bigcup_{1 \leq j \leq N} \bigcup_{t \in T_{ij}} QW_j + t^*$$

for $1 \leq i \leq N$. In this step, since the W_i are compact sets in \mathbb{R}^{d-1} , the union on the right-hand side need no longer be disjoint. By Banach's contraction principle, there is a unique solution to the IFS (9) within $(\mathcal{K}\mathbb{R}^{d-1})^N$; see [10, Thm. 1.1 and Prop. 1.3]. It is a well-known fact that the compact sets W_i can be Rauzy fractals with complicated topological structure and boundary [44, 45]; see [39, Sec. 7.4] and references therein for background. Note that Banach's contraction principle also gives us that each set A_i^* lies dense in the set W_i , which plays the role of a window for the CPS (5).

Remark 3.3. Let us briefly mention that Eq. (9) gives rise to a *dual inflation*, via multiplying from the left by Q^{-1} , which is an expansive mapping. This results in

$$Q^{-1}W_i = \bigcup_{1 \leq j \leq N} \bigcup_{t \in T_{ij}} W_j + Q^{-1}t^*,$$

where $Q^{-1}t^* = (t/\lambda)^*$. Iterating this rule in internal space either leads to a tiling or to a multiple cover of internal space, where the covering degree is constant almost everywhere. This follows from [45, Cor. 5.81], which extends an earlier idea from [25]. \diamond

Next, we recall a well-known result about the solution of the IFS (9), which can be seen as a special case of [45, Prop. 4.99]. Since it is of crucial importance to our further arguments, we also include a proof that is tailored to our setting. The latter considers primitive inflation tilings of \mathbb{R} , with a PV unit λ as inflation factor and natural lengths of the N intervals chosen such that all control point positions lie in $\mathbb{Z}[\lambda]$, but in no proper submodule of it.

Lemma 3.4. *Under our general assumptions, the solution (W_1, \dots, W_N) to the IFS (9) is row-wise measure-disjoint, which means that, for each $1 \leq i \leq N$, any two distinct sets on the right-hand side of (9) intersect at most in a Lebesgue-null set.*

Moreover, there is a number $\eta > 0$ such that $\text{vol}(W_i) = \eta v_i$ holds for all $1 \leq i \leq N$, where v_i is the relative frequency of the tiles of type i .

Proof. All W_i are compact sets, hence measurable, with $\text{vol}(W_i) \geq 0$. Let Λ_i be the set of control points of type i for one of the typed point sets $\Lambda = \bigcup_i \Lambda_i$ that emerge from the limit cycle of the iteration (8), as explained in Remark 3.2. By construction, due to the properties of the \star -map, we then know that $\Lambda_i \subseteq \mathcal{L}(W_i) := \{x \in L : x^* \in W_i\}$, where Λ_i is linearly repetitive, with $\text{dens}(\Lambda_i) = v_i \text{dens}(\Lambda) > 0$. Consequently, by [24, Prop. 3.4], which is an extension of the density result [43, Thm. 1] for regular model sets to the more general setting of weak model sets, we know that

$$0 < \text{dens}(\Lambda_i) \leq \underline{\text{dens}}(\mathcal{L}(W_i)) \leq \text{dens}(\mathcal{L}) \text{vol}(W_i),$$

where $\underline{\text{dens}}$ refers to the (always existing) lower density of a point set. This estimate means that we have $\text{vol}(W_i) > 0$ for all $1 \leq i \leq N$.

Now, due to a potential overlap of sets on the right-hand side of Eq. (9), one has

$$(10) \quad \text{vol}(W_i) \leq |\det(Q)| \sum_{j=1}^N \text{card}(T_{ij}) \text{vol}(W_j), \quad \text{for } 1 \leq i \leq N.$$

Observing $|\det(Q)| = \lambda^{-1}$ and $\text{card}(T_{ij}) = M_{ij}$, this amounts to the vector inequality

$$M|w\rangle \geq \lambda|w\rangle,$$

where $|w\rangle$ denotes the vector with entries $\text{vol}(W_i)$ and the inequality holds for each component. Since λ is the PF eigenvalue of M , which is primitive, and all entries of $|w\rangle$ are positive, we see that $|w\rangle$ is a positive multiple of the right PF eigenvector of M .

This means we have equality in (10), which implies the first claim, while the second is a consequence of $|w\rangle$ being proportional to $|v\rangle$. \square

All mappings that occur in our IFS (9) are of the form $x \mapsto Qx + u$, and hence homeomorphisms of \mathbb{R}^{d-1} . Invoking parts (i) and (iii) of [45, Prop. 4.99], one obtains the following improvement of Lemma 3.4.

Proposition 3.5. *Let (W_1, \dots, W_N) be the solution of the IFS (9). Then, under our assumptions, each $W_i \subset \mathbb{R}^{d-1}$ is a perfect, topologically regular set of positive Lebesgue measure. Moreover, each boundary ∂W_i has Lebesgue measure 0.* \square

In view of this result, all $\mathcal{A}(W_i)$ are *regular model sets* for the cut and project scheme $(\mathbb{R}, \mathbb{R}^{d-1}, \mathcal{L})$, see [35, 6] for background, hence also $\mathcal{A}(W) =$ with $W = \bigcup_i W_i$. The corresponding dynamical system (\mathbb{X}, \mathbb{R}) , where \mathbb{X} is the orbit closure of $\mathcal{A}(W)$ in the local topology and \mathbb{R} acts by translation, has pure point spectrum, both in the diffraction and in the dynamical sense; see [6, 8, 9] and references therein. The same property holds for the systems built from the translation orbit closure of any of the $\mathcal{A}(W_i)$.

Remark 3.6. If we consider the weighted Dirac comb $\omega = \sum_i h_i \delta_{\Lambda_i}$ with $h_i \in \mathbb{C}$, the Bombieri–Taylor property for primitive inflation rules [5, Thm. 3.23 and Rem. 3.24], which is an extension of the results of [30] to the typed point sets emerging from a primitive inflation rule, implies the existence of coefficients $A_i(k)$, called scattering or diffraction *amplitudes*, such that ω has the *diffraction measure*

$$(11) \quad \widehat{\gamma}_\omega = \sum_{k \in L^\circledast} I(k) \delta_k \quad \text{with} \quad I(k) = \left| \sum_i h_i A_i(k) \right|^2,$$

where L^\circledast is the projection of \mathcal{L}^* into \mathbb{R} as in Remark 3.1.

Now, assume in addition that $\mathcal{A}(W_i^\circ) \subseteq \Lambda_i \subseteq \mathcal{A}(W_i)$ holds for all $1 \leq i \leq N$, with the W_i from the solution of (9). Then, our typed point set $\Lambda = \bigcup_i \Lambda_i$ consists of disjoint, regular model sets. Consequently, by the general theory of model sets [35, 6], the amplitudes $A_i(k)$ for $k \in L^\circledast$ are given by

$$(12) \quad A_i(k) = \frac{\text{dens}(\Lambda_i)}{\text{vol}(W_i)} \widetilde{1_{W_i}}(k^\star) = \frac{\text{dens}(\Lambda)}{\text{vol}(W)} \widetilde{1_{W_i}}(k^\star),$$

where 1_K is the characteristic function of K and $\widetilde{\cdot}$ denotes inverse Fourier transform. For all other k , one has $A_i(k) = 0$. As we shall see later, a more general connection is possible via the Fourier–Bohr coefficients of Λ and its subsets; see Eq. (19) below for more. Note that the validity of (12) is a consequence of the uniform distribution of Λ_i^\star in W_i ; compare the detailed discussions in [6, Sec. 7.1] and [43]. \diamond

Though Eq. (12) looks nice, it is generally difficult to calculate $\widetilde{1_{W_i}}$ directly, due to the potentially fractal nature of the window boundaries. Let us thus turn to an alternative approach of transfer matrix type that harvests the inflation nature of our point sets. In view

of Lemma 3.4, Eq. (9) can now be rewritten as

$$(13) \quad 1_{W_i} = \sum_{j=1}^N \sum_{t \in T_{ij}} 1_{QW_j+t^*},$$

to be understood in the Lebesgue sense (rather than pointwise).

Theorem 3.7. *Let $(W_1, \dots, W_N) \in (\mathcal{K}\mathbb{R}^{d-1})^N$ be the unique solution to the contractive IFS (9). Then, Eq. (13) holds in the Lebesgue sense for every $1 \leq i \leq N$.*

Moreover, when considering the compact set $W = \bigcup_i W_i$, one has

$$\sum_{i=1}^N 1_{W_i}(y) = \mathbf{m}_c(y) 1_W(y),$$

where \mathbf{m}_c is a measurable function with $\text{supp}(\mathbf{m}_c) = W$ and values in $\{1, 2, \dots, N\}$ for $y \in W$.

Proof. The validity of (13) in the Lebesgue sense is clear from Lemma 3.4.

Since all W_i are compact, the function \mathbf{m}_c is well defined for all $y \in W$ and also measurable on W , as follows from a standard inclusion-exclusion argument with the (finitely many) compact sets W_i . This also gives $\mathbf{m}_c(y) \in \{1, \dots, N\}$ for each $y \in W$. \square

Remark 3.8. Under some additional conditions, \mathbf{m}_c is constant for almost every $y \in W$, with integer value m_c . In this case, one has $\sum_{i=1}^N \text{vol}(W_i) = m_c \text{vol}(W)$. This situation happens whenever the inflation defines a model set, where $m_c = 1$. Beyond this case, one can have integer values of m_c , possibly up to $N - 1$.

In general, however, \mathbf{m}_c need not be constant almost everywhere in the total window W , as we shall see in the example from Eq. (24) in Section 7. This seems a significant difference to the covering degree of internal space by the dual inflation mentioned in Remark 3.3. We shall return to this point in Section 5. \diamond

Let us now switch to an analysis of the system (13) of equations after (inverse) Fourier transform, which turns it into a rescaling equation for an N -tuple of continuous functions.

4. ANALYSIS OF INTERNAL COCYCLE

Let us first recall a simple, but in our context vital, result on the inverse Fourier transform of characteristic functions, which we prove for convenience.

Lemma 4.1. *Let $m \in \mathbb{N}$ be fixed. Let $K \subset \mathbb{R}^m$ be compact and $Q \in \text{GL}(m, \mathbb{R})$. Then, one has the relation*

$$\widetilde{1_{QK+t}}(y) = |\det(Q)| e^{2\pi i \langle t, y \rangle} \widetilde{1_K}(Q^T y),$$

which holds for all $t, y \in \mathbb{R}^m$, with continuity in both variables.

Proof. With the change of variable $x = Qu + t$, one finds

$$\begin{aligned} \widetilde{1_{QK+t}}(y) &= \int_{QK+t} e^{2\pi i \langle x|y \rangle} dx = |\det(Q)| e^{2\pi i \langle t|y \rangle} \int_K e^{2\pi i \langle Qu|y \rangle} du \\ &= |\det(Q)| e^{2\pi i \langle t|y \rangle} \int_K e^{2\pi i \langle u|Q^T y \rangle} du = |\det(Q)| e^{2\pi i \langle t|y \rangle} \widetilde{1_K}(Q^T y). \end{aligned}$$

Continuity in y follows from the Fourier transform of an L^1 -function being continuous, see [42, Thm. IX.7], while continuity in t is obvious. \square

Fix $m = d - 1$ and let Q now be the linear map in internal space that is induced by the dilation $x \mapsto \lambda x$ in direct space, as given in (6). Set $f_i(y) := \widetilde{1_{W_i}}(y)$ and consider the vector $|f(y)\rangle = |f_1(y), \dots, f_N(y)\rangle$. Also, let $\underline{B}(y)$ be the *internal Fourier matrix* that emerges from the (inverse) Fourier transform of the \star -image of the displacement matrix T , that is,

$$\underline{B}_{ij}(y) = \sum_{x \in T_{ij}} e^{2\pi i \langle x^*|y \rangle},$$

with $y \in \mathbb{R}^{d-1}$. The matrix elements are again trigonometric polynomials, this time generally multivariate. Now, with Lemma 4.1 and $|\det(Q)| = \lambda^{-1}$, one finds the following result of transfer matrix type via an elementary computation; compare [38, Sec. 3.2] for a mathematically similar structure.

Proposition 4.2. *Under inverse Fourier transform, Eq. (13) becomes*

$$|f(y)\rangle = \lambda^{-1} \underline{B}(y) |f(Ry)\rangle,$$

with $R = Q^T$ and $\underline{B}(y) = \widetilde{\delta_{T^*}}(y)$ as defined above, and all f_i continuous. \square

It is clear that $\lim_{y \rightarrow 0} \underline{B}(y) = \underline{B}(0) = M$. Moreover, from the way it was constructed, we know that R is a normal matrix and a contraction. Consequently, its spectral norm agrees with its spectral radius, see [23, Sec. 2.3], and we have $\theta := \|R\|_2 = \rho(R) < 1$. This leads to the following property, where we use $\|\cdot\|_2$ also for the 2-norm of vectors.

Lemma 4.3. *For any $\varepsilon > 0$, there exists $\delta = \delta(\varepsilon) > 0$ such that*

$$\|\underline{B}(R^m y) - M\|_2 < \theta^m \varepsilon$$

holds simultaneously for all $\|y\|_2 < \delta$ and all $m \in \mathbb{N}$.

Proof. Since each element of $\underline{B}(y)$ is analytic, one has the expansions

$$\underline{B}_{ij}(y) = M_{ij} + \langle u_{ij}|y \rangle + \mathcal{O}(\|y\|_2^2)$$

near the origin, with $u_{ij} = \nabla \underline{B}_{ij}(0)$, which are N^2 fixed vectors. Consequently, using $\|R^m y\|_2 \leq \|R^m\|_2 \|y\|_2 \leq \|R\|_2^m \|y\|_2 = \theta^m \|y\|_2$ and the Cauchy–Schwarz inequality, we get

$$|\underline{B}_{ij}(R^m y) - M_{ij}| \leq \theta^m \|u_{ij}\|_2 \|y\|_2 + \theta^{2m} \mathcal{O}(\|y\|_2^2),$$

from which the claim follows by standard arguments. \square

Now, for $n \in \mathbb{N}$, we can define an *internal cocycle* from the Fourier matrix via

$$\underline{B}^{(n)}(y) := \underline{B}(y)\underline{B}(Ry) \cdots \underline{B}(R^{n-1}y),$$

with $\underline{B}^{(1)} = \underline{B}$ and $\underline{B}^{(n)}(0) = M^n$. In analogy to (4), we now have

$$(14) \quad \underline{B}^{(n+1)}(y) = \underline{B}^{(n)}(y)\underline{B}(R^n y) = \underline{B}(y)\underline{B}^{(n)}(Ry)$$

for all $n \geq 1$. Next, we want to consider the matrix function defined by

$$(15) \quad C(y) := \lim_{n \rightarrow \infty} \beta^n \underline{B}^{(n)}(y),$$

with $\beta = |\det(R)|$, where $\beta\lambda = 1$ because λ is a unit. We thus need to establish that $C(y)$ is well defined as a limit, for every $y \in \mathbb{R}^{d-1}$. To this end, we employ the 2-norm for vectors and the corresponding operator norm, both denoted by $\|\cdot\|_2$ as before.

Proposition 4.4. *The sequence $(\beta^n(\underline{B}^{(n)}(y) - M^n))_{n \in \mathbb{N}}$ of matrix functions is equicontinuous at $y = 0$, which is to say that*

$$\forall \varepsilon > 0: \exists \delta = \delta(\varepsilon) > 0: \forall n \in \mathbb{N}: (\|y\|_2 < \delta \implies \beta^n \|\underline{B}^{(n)}(y) - M^n\|_2 < \varepsilon).$$

Proof. Since M is non-negative, the spectral radius of M^n is $\rho(M^n) = \lambda^n$, for all $n \in \mathbb{N}_0$. Let us first consider the case that M is normal. Then, we can most easily work with the spectral norm, because we have $\|M^n\|_2 = \rho(M^n) = \lambda^n$ for $n \geq 0$, hence $\|M^n\|_2 = \|M\|_2^n$. Also, we get

$$\|\underline{B}(y)\|_2 \leq \| |\underline{B}(y)| \|_2 \leq \|M\|_2$$

for all y in this case. This estimate holds because the spectral norm has the required monotonicity property; compare [26, Thm. 1] or [22, Exc. 5.6.P42].

Now, harvesting the cocycle property (14), a simple telescopic argument leads to

$$\underline{B}^{(n)}(y) - M^n = \sum_{\ell=0}^{n-1} M^\ell (\underline{B}(R^\ell y) - M) \underline{B}^{(n-1-\ell)}(R^{\ell+1}y)$$

for $n \geq 1$, with $\underline{B}^{(0)} := \mathbb{1}$. Via the triangle inequality, using the above properties, one then finds the estimate

$$\|\underline{B}^{(n)}(y) - M^n\|_2 \leq \|M\|_2^{n-1} \sum_{\ell=0}^{n-1} \|\underline{B}(R^\ell y) - M\|_2 = \lambda^{n-1} \sum_{\ell=0}^{n-1} \|\underline{B}(R^\ell y) - M\|_2.$$

For $\varepsilon > 0$ and $\|y\|_2 < \delta$, with $\beta = \lambda^{-1}$ and the δ from Lemma 4.3, this gives

$$\|\beta^n(\underline{B}^{(n)}(y) - M^n)\|_2 \leq \beta \sum_{\ell=0}^{n-1} \theta^\ell \varepsilon \leq \frac{\beta \varepsilon}{1 - \theta}$$

by a geometric series argument, which establishes the claim when M is normal.

For the general case, we employ a different sub-multiplicative matrix norm, which depends on M and again satisfies $\|M\| = \rho(M)$, hence $\|M^n\| \leq \|M\|^n = \lambda^n$. Following [23, Sec. 2.4], one such norm can simply be constructed as follows. Consider the convex body

$$K = \text{diag}(v_1, \dots, v_N) \{x \in \mathbb{C}^N : \|x\|_\infty \leq 1\},$$

where the v_i are the strictly positive entries of $|v\rangle$, the (frequency normalised) right PF eigenvector of M , and define

$$\|x\|_v := \inf \{ \alpha > 0 : x \in \alpha K \} = \max_{1 \leq i \leq N} \frac{|x_i|}{v_i}.$$

This is a matrix norm on \mathbb{C}^N that is *absolute*, so $\|x\|_v = \||x|\|_v$ for all $x \in \mathbb{C}^N$, with $|x|$ denoting the vector with entries $|x_i|$. Now, let $\|\cdot\|_K$ denote the matching operator norm on $\text{Mat}(N, \mathbb{C})$, as defined by

$$\|A\|_K := \sup_{\|x\|_v=1} \|Ax\|_v,$$

which is sub-multiplicative and satisfies $\|M\|_K = \rho(M) = \lambda$ by construction. What is more, it also satisfies the monotonicity property $\|A\|_K \leq \||A|\|_K$ for all $A \in \text{Mat}(N, \mathbb{C})$, again by [22, Thm. 1]. Consequently, we still get $\|\underline{B}^{(n)}(y)\|_K \leq \|M^n\|_K \leq \|M\|_K^n$ for all $y \in \mathbb{C}^{d-1}$ and all $n \in \mathbb{N}$.

Equipped with this matrix norm, we can repeat our previous telescopic argument, now leading to the estimate

$$\|\beta^n (\underline{B}^{(n)}(y) - M^n)\|_K \leq \beta \sum_{\ell=0}^{n-1} \|\underline{B}(R^\ell y) - M\|_K.$$

From here, since the vector norms $\|\cdot\|_2$ and $\|\cdot\|_v$ are equivalent, as are the matrix norms $\|\cdot\|_2$ and $\|\cdot\|_K$, we can adjust the choice of $\delta = \delta(\varepsilon)$ to reach the same conclusion. \square

Combining the equicontinuity of $\beta^n \underline{B}^{(n)}(y)$ at 0 from Proposition 4.4 with Fact 2.1, a standard 2ε -argument gives the following consequence.

Corollary 4.5. *Let P be the projector from (1) and $\underline{B}^{(n)}(y)$ the internal cocycle. Then, for all $\varepsilon > 0$, there exists $\delta' = \delta'(\varepsilon) > 0$ such that*

$$\|\beta^n \underline{B}^{(n)}(y) - P\|_2 < \varepsilon$$

holds for all $n \in \mathbb{N}$ and all $y \in \mathbb{R}^{d-1}$ with $\|y\|_2 < \delta'$. \square

Now, we are set to establish the convergence of our internal cocycle as follows.

Theorem 4.6. *The scaled cocycle sequence $(\beta^n \underline{B}^{(n)}(y))_{n \in \mathbb{N}}$ converges compactly on \mathbb{R}^{d-1} . Consequently, the matrix function $C(y)$ from (15) is well defined and continuous.*

Proof. Let $K \subset \mathbb{R}^{d-1}$ be compact, choose $\varepsilon > 0$, and let $\delta = \delta(\varepsilon) > 0$ be as in Proposition 4.4. We will establish the claim by showing that the sequence is uniformly Cauchy on K .

For $p, q, r \in \mathbb{N}$, we employ the cocycle property from (14) to get

$$\begin{aligned} (16) \quad & \|\beta^{p+q} \underline{B}^{(p+q)}(y) - \beta^{p+q+r} \underline{B}^{(p+q+r)}(y)\|_2 \\ & \leq \|\beta^p \underline{B}^{(p)}(y)\|_2 \|\beta^q \underline{B}^{(q)}(R^p y) - \beta^{q+r} \underline{B}^{(q+r)}(R^p y)\|_2, \end{aligned}$$

where the first factor on the right is bounded by $\beta^p \|M^p\|_2$ and thus uniformly bounded by a constant c_B , as a consequence of Fact 2.3 used with the spectral norm. Via the triangle inequality, the second factor on the right-hand side of (16) is bounded by

$$(17) \quad \|\beta^q (\underline{B}^{(q)}(R^p y) - M^q)\|_2 + \|\beta^q M^q - \beta^{q+r} M^{q+r}\|_2 + \|\beta^{q+r} (\underline{B}^{(q+r)}(R^p y) - M^{q+r})\|_2.$$

Choose p large enough so that $R^p K$ is contained in the open ball of radius δ around 0, which is possible because R is a contraction. Then, the first term in (17), as well as the last, is bounded by ε . Since $(\beta^n M^n)_{n \in \mathbb{N}}$ converges to P by Fact 2.1, where $\beta = \lambda^{-1}$, the sequence is Cauchy, so there is a $q_0 \in \mathbb{N}$ such that the middle term in (17) is bounded by ε , for all $q \geq q_0$ and $r \in \mathbb{N}$. Consequently, (17) is bounded by 3ε for the chosen p , all $q \geq q_0$, and all $r \in \mathbb{N}$. Via Fact 2.3, this gives an upper bound of $3c_B \varepsilon$ to the left-hand side of (16). As this bound is independent of $y \in K$, and $\varepsilon > 0$ was arbitrary, uniform convergence on K follows.

Since we have a compactly convergent sequence of matrix functions, each of which is analytic and thus certainly continuous, the last claim is obvious. \square

Let us now analyse the matrix function $C(y)$, where we know

$$C(0) = P$$

from Fact 2.1. Now, Eq. (14) implies that, for any fixed $m \in \mathbb{N}$,

$$C(y) = \lim_{n \rightarrow \infty} \beta^{n+m} \underline{B}^{(n+m)}(y) = C(y) \beta^m \lim_{n \rightarrow \infty} \underline{B}^{(m)}(R^n y) = C(y) \beta^m M^m,$$

because R is a contraction and $\underline{B}^{(m)}(0) = M^m$. With $m = 1$, this gives

$$C(y)M = \lambda C(y),$$

as well as $C(y) = C(y)P$ from taking the limit $m \rightarrow \infty$. Each row of $C(y)$ thus is a left eigenvector of M for its eigenvalue λ , hence a y -dependent multiple of $\langle u |$, which means

$$(18) \quad C(y) = |c(y)\rangle \langle u|$$

with $|c(0)\rangle = |v\rangle$. Observing that the window volumes are proportional to the entries of $|v\rangle$ by Lemma 3.4, so $|f(0)\rangle = \eta|v\rangle$ for some $\eta > 0$, one has the following consequence.

Corollary 4.7. *For any $y \in \mathbb{R}^{d-1}$, the matrix $C(y)$ from (15) has rank 1, and can be represented as in (18). Moreover, with $f_i = \widetilde{1_{W_i}}$, one has $|f(y)\rangle = \eta|c(y)\rangle$ together with $|c(y)\rangle = C(y)|v\rangle$. \square*

In particular, this result makes the functions f_i effectively computable from C .

Remark 4.8. Let us mention that the continuity of the functions f_i is also clear from the fact that each is the (inverse) Fourier transform of an L^1 -function, and f_i decays at infinity by the Riemann–Lebesgue lemma; see [42, Thm. IX.7]. What is more, since all W_i are compact, we actually know that each f_i has an analytic continuation to an entire analytic function of $d-1$ variables, with a well-known growth estimate according to the Paley–Wiener theorem; see [42, Thm. IX.12] for details. \diamond

5. FOURIER–BOHR COEFFICIENTS AND UNIFORM DISTRIBUTION

Here, we explain the general connection with the diffraction amplitudes mentioned earlier in Remark 3.6. Given a typed point set $\Lambda = \bigcup_i \Lambda_i \subset \mathbb{R}$, its *Fourier–Bohr (FB) coefficient* (or amplitude) at $k \in \mathbb{R}$ is defined as a volume-averaged exponential sum,

$$(19) \quad A_\Lambda(k) := \lim_{r \rightarrow \infty} \frac{1}{2r} \sum_{\substack{x \in \Lambda \\ |x| \leq r}} e^{-2\pi i k x},$$

and similarly for the control point sets Λ_i with $1 \leq i \leq N$, provided the limits exist. This is the case for point sets from primitive inflation rules, which are linearly repetitive and thus uniquely ergodic [48, 27]. The definition entails that $A_\Lambda(0) = \text{dens}(\Lambda)$, and one gets $\sum_{i=1}^N A_{\Lambda_i}(k) = A_\Lambda(k)$ for all $k \in \mathbb{R}$ because the point sets Λ_i are disjoint by construction.

In general, we know from the embedding procedure that $\overline{\Lambda_i^*} = W_i$. If Λ_i is also a model set, the point set Λ_i^* is uniformly distributed (and even well distributed) in W_i ; compare [43]. This uniform distribution occurs more generally, as we analyse next.

It is clear from Remark 3.8 and the example in Section 7 that the lift of Λ to internal space will not be uniformly distributed in W in general. However, the situation is more favourable for the individual point sets Λ_i . For any $1 \leq i \leq N$, consider the sequence $(\mu_i^{(n)})_{n \in \mathbb{N}}$ of point measures in internal space defined by

$$\mu_i^{(n)} = \frac{1}{2n} \sum_{\substack{x \in \Lambda_i \\ |x| \leq n}} \delta_{x^*}.$$

Clearly, one has $\text{supp}(\mu_i^{(n)}) \subset W_i$ by construction, and $\mu_i := \lim_{n \rightarrow \infty} \mu_i^{(n)}$ exists (under weak convergence), due to the strict ergodicity of the dynamical system defined by Λ_i . An explicit argument for this convergence, based on the linear repetitivity of Λ_i , can be formulated along the lines of the proof of [27, Thm. 5.1]. Here, μ_i is a positive measure on \mathbb{R}^{d-1} with $\text{supp}(\mu_i) \subseteq W_i$ and total mass $\|\mu_i\| = \text{dens}(\Lambda_i)$. We say that Λ_i *induces* the measure μ_i in internal space.

When Λ_i induces μ_i , a simple calculation (with a change of the summation variable) shows that $\lambda \Lambda_i + t$ with $t \in \mathbb{Z}[\lambda]$ induces the positive measure

$$\frac{1}{\lambda} \delta_{t^*} * (Q \cdot \mu_i),$$

where Q is the contraction from (6) and $Q \cdot \mu$ denotes the push-forward of a finite measure μ , so $(Q \cdot \mu)(\varphi) = \mu(\varphi \circ Q)$ for $\varphi \in C_0(\mathbb{R}^{d-1})$. Equivalently, one can use $(Q \cdot \mu)(\mathcal{E}) = \mu(Q^{-1}(\mathcal{E}))$ with \mathcal{E} an arbitrary Borel set.

Let us now assume that our typed point set $\Lambda = \bigcup_i \Lambda_i$ is a fixed point of the inflation equation (8). This is no restriction as one can always achieve this via replacing ϱ by a suitable power; compare Remark 3.2. Then, our induced measures μ_1, \dots, μ_N must satisfy

$$(20) \quad \mu_i = \frac{1}{\lambda} \sum_{j=1}^N \sum_{t \in T_{ij}} \delta_{t^*} * (Q \cdot \mu_j),$$

which defines a system of N linear equations. We can spell out one solution as follows, where $\lambda_{\mathbb{L}}$ denotes Lebesgue measure on internal space.

Lemma 5.1. *The absolutely continuous measures $\mu_i = g_i \lambda_{\mathbb{L}}$ with Radon–Nikodym densities*

$$g_i = \frac{\text{dens}(\Lambda_i)}{\text{vol}(W_i)} 1_{W_i}$$

satisfy (20) together with $\|\mu_i\| = \text{dens}(\Lambda_i)$.

Proof. Observe that $Q \cdot (1_{W_i} \lambda_{\mathbb{L}}) = |\det(Q)|^{-1} 1_{QW_i} \lambda_{\mathbb{L}}$, which follows from a simple change of variable calculation. Likewise, one has $\delta_{t^*} * 1_{W_i} = 1_{W_i+t^*}$, and inserting the ansatz into (20) leads to

$$\frac{\text{dens}(\Lambda_i)}{\text{vol}(W_i)} 1_{W_i} = \sum_{j=1}^N \sum_{t \in T_{ij}} \frac{\text{dens}(\Lambda_j)}{\text{vol}(W_j)} 1_{QW_j+t^*}.$$

By construction, we have $\text{dens}(\Lambda_i) = \text{dens}(\Lambda) v_i$, where v_i is the relative frequency of points of type i ; compare Remark 2.2. On the other hand, we know from Lemma 3.4 that the N window volumes satisfy $\text{vol}(W_i) = \eta v_i$ for some fixed $\eta > 0$, which implies that

$$\frac{\text{dens}(\Lambda_i)}{\text{vol}(W_i)} = \frac{\text{dens}(\Lambda)}{\eta}$$

is independent of i , and the previous equation turns into the window equation (13), which is satisfied in the Lebesgue sense.

The claimed normalisation is obvious. \square

Now, we interpret the right-hand side of (20) as a linear mapping on $(\mathcal{M}_+(\mathbb{R}^{d-1}))^N$, with $\mathcal{M}_+(\mathbb{R}^{d-1})$ denoting the finite, positive measures on \mathbb{R}^{d-1} , equipped with the total variation norm, $\|\cdot\|$. If (μ_1, \dots, μ_N) is an N -tuple of positive measures, its image is (μ'_1, \dots, μ'_N) with

$$\begin{aligned} \|\mu'_i\| &= \left\| \frac{1}{\lambda} \sum_{j=1}^N \sum_{t \in T_{ij}} \delta_{t^*} * (Q \cdot \mu_j) \right\| = \frac{1}{\lambda} \sum_{j=1}^N \sum_{t \in T_{ij}} \|\delta_{t^*} * (Q \cdot \mu_j)\| \\ &= \frac{1}{\lambda} \sum_{j=1}^N M_{ij} \|Q \cdot \mu_j\| = \frac{1}{\lambda} \sum_{j=1}^N M_{ij} \|\mu_j\|. \end{aligned}$$

Consequently, when $\|\mu_i\| = \alpha v_i$ for all $1 \leq i \leq N$ and some $\alpha > 0$, the total mass of each μ_i is preserved under the iteration because $M|v\rangle = \lambda|v\rangle$. This leads to the following result.

Proposition 5.2. *Let $\alpha > 0$ be fixed and consider the space*

$$\mathcal{M}_\alpha := \{(\nu_1, \dots, \nu_N) : \nu_i \in \mathcal{M}_+(\mathbb{R}^{d-1}), \|\nu_i\| = \alpha v_i\},$$

with $|v\rangle$ the right PF eigenvector of M . Then, \mathcal{M}_α is invariant under the iteration of the right-hand side of (20), and contains precisely one solution to Eq. (20), namely the one defined by $\nu_i = \frac{\alpha v_i}{\text{vol}(W_i)} 1_{W_i} \lambda_{\mathbb{L}}$ for $1 \leq i \leq N$.

Proof. The space \mathcal{M}_α can be equipped with the Hutchinson metric, compare [10, Sec. 2] and references therein, which turns it into a complete metric space. The iteration then is a contraction, as is obvious from the estimate

$$\left\| \frac{1}{\lambda} \delta_{t^*} * (Q \cdot \mu_j) \right\| = \frac{1}{\lambda} \|\delta_{t^*} * (Q \cdot \mu_j)\| = \frac{1}{\lambda} \|Q \cdot \mu_j\| = \frac{1}{\lambda} \|\mu_j\|$$

where $\lambda > 1$; see [10, Sec. 5] for the remaining steps.

Now, the first claim is a consequence of Banach's contraction principle, while the concrete form of the solution follows from Lemma 5.1. \square

If one starts the iteration with an arbitrary N -tuple of non-negative measures, not all 0, there is a unique component of the total mass vector in the PF direction of M , which defines the parameter α , and all other components decay exponentially fast.

Our main result of this section can now be formulated as follows.

Theorem 5.3. *Let $\Lambda = \bigcup_i \Lambda_i$ be the typed point set of a primitive, unimodular PV inflation rule as constructed above, and consider the natural CPS that emerges from the Minkowski embedding. Then, each Λ_i induces a unique measure in internal space, namely*

$$\mu_i = \frac{\text{dens}(\Lambda_i)}{\text{vol}(W_i)} \mathbf{1}_{W_i} \lambda_L,$$

where the W_i are the solutions of the window IFS (9). This entails the statement that, for all $1 \leq i \leq N$, the set Λ_i^* is uniformly distributed in W_i .

Proof. The IFS (20) for the distributions induced by the Λ_i on the compact sets W_i is contractive on \mathcal{M}_α , with $\alpha = \text{dens}(\Lambda)$, and the unique solution is the one stated.

Recalling the definition of the induced measures, weak convergence clearly is equivalent to the uniform distribution of Λ_i^* in W_i . \square

At this point, we can return to the connection between the FB coefficients and the Fourier transform of the windows, even though the latter generally only code a covering model set. Still, due to uniform distribution, for $k \in L^\otimes$, one obtains an explicit formula, namely

$$A_{\Lambda_i}(k) = \frac{\text{dens}(\Lambda_i)}{\text{vol}(W_i)} \widetilde{\mathbf{1}_{W_i}}(k^*),$$

together with $A_{\Lambda_i}(k) = 0$ for any $k \in \mathbb{R} \setminus L^\otimes$. If, in addition, the function \mathfrak{m}_c from Remark 3.8 satisfies $\mathfrak{m}_c(y) = m_c$ for a.e. $y \in W$, one also gets

$$(21) \quad A_{\Lambda_i}(k) = \frac{\text{dens}(\mathcal{L})}{m_c} \widetilde{\mathbf{1}_{W_i}}(k^*).$$

Remark 5.4. If we interpret the Fourier–Bohr coefficient $A_\Lambda(k)$ as a function of Λ , one obtains

$$A_{t+\Lambda}(k) = e^{-2\pi i k t} A_\Lambda(k).$$

Consequently, whenever the coefficient does not vanish, this defines an eigenfunction of the strictly ergodic dynamical system (\mathbb{Y}, \mathbb{R}) , where \mathbb{Y} is the hull of Λ obtained as the closure of the translation orbit $\{t + \Lambda : t \in \mathbb{R}\}$ in the local topology; compare [6, Ch. 4]. The analogous

connection exists with the A_{A_i} for $1 \leq i \leq N$, not all of which can vanish simultaneously for any given $k \in L^\otimes$. This explains why L^\otimes is the pure point part of the dynamical spectrum (in additive notation) and how the diffraction intensities are connected with the eigenfunctions; see [9, 30] and references therein for more.

Both for regular model sets and for primitive inflation tilings, it is known that the eigenfunctions are continuous on \mathbb{Y} ; see [30] and references therein. This also means that the dynamical point spectrum for such systems is the same in the topological and in the measure-theoretic sense. \diamond

Whenever constant covering of the total window is satisfied in our setting, we have the following consequence for the Fourier–Bohr coefficients.

Corollary 5.5. *Assume that the total window covering is almost surely constant. Then, the Fourier–Bohr coefficients, for $k \in L^\otimes$, are obtained as*

$$A_{A_i}(k) = \text{dens}(\Lambda) c_i(k^*),$$

and vanish for all other k . \square

The corresponding diffraction intensities follow from Eq. (11). Note that the covering degree does *not* show up in this relation. The intensity at any wave number $k \in L^\otimes$ can be efficiently approximated by truncating the infinite product representation for $C(k^*)$ and calculating the amplitudes as explained above.

At this point, we turn to some applications of the cocycle method to concrete inflation systems on the real line.

6. EXAMPLES – THE PISA SUBSTITUTIONS

Let us introduce an interesting family of primitive inflations as follows, based on the alphabet $\mathcal{A} = \{a_1, \dots, a_d\}$ with $d \geq 2$. The explicit rule is given by $a_i \mapsto a_1 a_{i+1}$ for $1 \leq i \leq d-1$, together with $a_d \mapsto a_1$. In short, we have $\varrho_d = (a_1 a_2, a_1 a_3, \dots, a_1 a_d, a_1)$. We call $\{\varrho_d : d \geq 2\}$ the family of *Pisa substitutions*. For $d = 2$, this is the classic Fibonacci rule, while $d = 3$ is known as the Tribonacci substitution in the literature; see [39] and references therein.

Let us first collect some general results for this family. The substitution matrix reads

$$M_d = \begin{pmatrix} 1 & 1 & 1 & \dots & 1 & 1 \\ 1 & 0 & 0 & \dots & 0 & 0 \\ 0 & 1 & 0 & \dots & 0 & 0 \\ 0 & 0 & 1 & \dots & 0 & 0 \\ \vdots & \vdots & & \ddots & & \vdots \\ 0 & 0 & 0 & \dots & 1 & 0 \end{pmatrix}$$

with $\det(M_d) = (-1)^{d-1}$. Note that M_d is not normal for $d \geq 3$, whence we need Proposition 4.4 in the generality stated and proved. The characteristic polynomial of M_d is

$$p_d(x) = x^d - (1 + x + x^2 + \dots + x^{d-1}).$$

By [13, Thm. 2], p_d is irreducible, with one root > 1 , which is the PF eigenvalue λ_d of M_d , and all others inside the unit disc. So, λ_d is a PV unit of degree d , which satisfies $\lim_{d \rightarrow \infty} \lambda_d = 2$. The discriminant of p_d for $d \geq 2$ is given by

$$\Delta_d = (-1)^{\frac{d(d+1)}{2}} \frac{(d+1)^{d+1} - 2(2d)^d}{(d-1)^2},$$

which is due to M. Alekseyev; see [47, A106273] for details.

The right PF eigenvector is denoted by $|v\rangle$ as before, where we now drop the dependence on d for ease of notation. When normalised as $\langle 1|v\rangle = 1$, it reads

$$|v\rangle = (\lambda^{-1}, \lambda^{-2}, \lambda^{-3}, \dots, \lambda^{-d+1}, \lambda^{-d})^T.$$

The corresponding left PF eigenvector $\langle u|$ is normalised such that $\langle u|v\rangle = 1$, which gives

$$\langle u| = \frac{\lambda^d - \lambda}{2\lambda^d - (d+1)\lambda + (d-1)} \left(\lambda, \sum_{j=0}^{d-2} \lambda^{-j}, \sum_{j=0}^{d-3} \lambda^{-j}, \dots, 1 + \lambda^{-1}, 1 \right).$$

Here, the normalisation prefactor was simplified via the algebraic relation for λ from $p(\lambda) = 0$. Note that the vector on the right-hand side is a canonical choice for the natural interval lengths, which all lie in $\mathbb{Z}[\lambda]$. The shortest interval then has length 1, and it is straightforward to show that no proper submodule of $\mathbb{Z}[\lambda]$ contains all control point positions. Here, the density of the resulting point set Λ is given by

$$\text{dens}(\Lambda) = \frac{\lambda^d - \lambda}{2\lambda^d - (d+1)\lambda + (d-1)},$$

with $\lim_{d \rightarrow \infty} \text{dens}(\Lambda) = \frac{1}{2}$.

When working with the \mathbb{Z} -module $L = \mathbb{Z}[\lambda]$, one can define the dual module L^{\otimes} with respect to the quadratic form $\text{tr}(xy)$ as explained in Remark 3.1, namely

$$(22) \quad L^{\otimes} = \{y \in \mathbb{Q}(\lambda) : \text{tr}(xy) \in \mathbb{Z} \text{ for all } x \in L\}.$$

For our family, one finds $L^{\otimes} = \vartheta L$ with

$$\vartheta = \left(d\lambda^{d-1} - \sum_{m=0}^{d-2} (m+1)\lambda^m \right)^{-1} \in \frac{1}{\Delta_d} \mathbb{Z}[\lambda].$$

We are now set to look at some special cases in more detail.

6.1. The Fibonacci tiling. For $\varrho_2 = (ab, a)$, which we write with the binary alphabet $\mathcal{A} = \{a, b\}$ for simplicity, the inflation tiling with interval lengths $\tau = \frac{1}{2}(1 + \sqrt{5})$ for a and 1 for b is well studied; see [6, Sec. 9.4.1] and references therein. For the standard fixed point of the square of ϱ_2 , with central seed $a|a$, one obtains the windows $W_a = (\tau - 2, \tau - 1]$ and $W_b = (-1, \tau - 2]$, compare [6, Ex. 7.3], and can calculate their Fourier transforms immediately. With $\text{sinc}(z) = \frac{\sin(z)}{z}$, they read

$$\widetilde{1_{W_a}}(y) = e^{\pi i y(2\tau-3)} \text{sinc}(\pi y) \quad \text{and} \quad \widetilde{1_{W_b}}(y) = \frac{e^{\pi i y(\tau-3)}}{\tau} \text{sinc}\left(\frac{\pi y}{\tau}\right).$$

Here, it does not matter whether we take open, half-open or closed intervals, as their characteristic functions are equal as L^1 -functions. Consequently, this detail is spectrally invisible.

The internal Fourier matrix and cocycle for this example read

$$\underline{B}(y) = \begin{pmatrix} 1 & 1 \\ e^{2\pi i \sigma y} & 0 \end{pmatrix} \quad \text{and} \quad \underline{B}^{(n)}(y) = \underline{B}(y)\underline{B}(\sigma y) \cdots \underline{B}(\sigma^{n-1}y),$$

with³ $\sigma = \tau^* = 1 - \tau$, so $|\sigma| = -\sigma$. We find the relation

$$c_b(y) = |\sigma| e^{2\pi i \sigma y} c_a(y)$$

expressing c_b in terms of c_a , while the latter is obtained as the limit

$$c_a(y) = \lim_{n \rightarrow \infty} q_n(y),$$

where the trigonometric polynomials q_n are recursively defined by

$$q_{n+1}(y) = |\sigma| q_n(\sigma y) + \sigma^2 e^{2\pi i \sigma^2 y} q_{n-1}(\sigma^2 y),$$

with initial conditions $q_1 = q_0 = |\sigma|$. From here, it is not difficult to check that

$$c_a(y) = |\sigma| \widetilde{1_{W_a}}(y) \quad \text{and} \quad c_b(y) = |\sigma| \widetilde{1_{W_b}}(y)$$

as it must. The convergence of the recursive formula for c_a is exponentially fast. Though there is no need for this alternative approach in this case, it provides a consistency check and some additional insight on the recursive structure of the spectrum.

6.2. (Twisted) Tribonacci. Here, we compare two different substitution rules for $d = 3$, which share the same substitution matrix $M = M_3$. These are the Tribonacci substitution $\varrho_3 := (ab, ac, a)$ and its twisted counterpart, $\varrho'_3 := (ba, ac, a)$. Note that further permutations of letter positions do not define new hulls, as they are conjugate to one of these two. Both lead to inflation systems that have fractal windows in their model set description, as they must due to a result by Pleasants [37, Prop. 2.35], but the twisted version is much more tortuous; see Figure 1 below, and compare [39, Figs. 7.5 and 7.8], where a different coordinate system is used. The fundamental group of the windows in the twisted case is huge, while the windows of the untwisted case are still simply connected, as also known from other examples such as the inflation tiling that underlies the Kolakoski-(3, 1) sequence [11].

The field $\mathbb{Q}(\lambda)$ is cubic. For ease of notation, we define $\kappa_{\pm} = (19 \pm 3\sqrt{33})^{\frac{1}{3}}$. With this, we find that the PF eigenvalue is

$$\lambda = \frac{1}{3}(1 + \kappa_+ + \kappa_-) \approx 1.839287.$$

The characteristic polynomial is cubic, $p(x) = x^3 - x^2 - x - 1$, with discriminant $\Delta = -44$. The remaining two eigenvalues form a complex conjugate pair $\alpha, \bar{\alpha}$ with $|\alpha|^2 = \lambda^{-1} = \lambda^2 - \lambda - 1$. This also gives $\lambda^{-2} = \lambda(2 - \lambda)$. Further, one finds $\text{Re}(\alpha) = (1 - \lambda)/2$ and $\text{Re}(\alpha^2) = (3 - \lambda^2)/2$,

³Here, σ is a number which should not be confused with the Galois isomorphisms from Section 3.

while $\operatorname{Im}(\alpha) = \frac{1}{2\sqrt{3}}(\kappa_+ - \kappa_-)$ and $\operatorname{Im}(\alpha^2) = (1 - \lambda)\operatorname{Im}(\alpha)$. From the discriminant and Vieta's theorem, one also gets

$$\operatorname{Im}(\alpha) = \frac{\sqrt{11}}{3\lambda^2 - 2\lambda - 1} = \frac{\sqrt{11}}{22}(-4\lambda^2 + 9\lambda + 1).$$

The natural tile lengths can be chosen as $(\lambda, \lambda^2 - \lambda, 1) \approx (1.839, 1.544, 1)$, which means that all control point positions lie in the rank-3 \mathbb{Z} -module $L = \langle 1, \lambda, \lambda^2 \rangle_{\mathbb{Z}}$, but in no proper submodule. The lattice for the CPS, \mathcal{L} , is obtained from the Minkowski embedding of L into 3-space. A canonical choice for the basis matrix of \mathcal{L} and its dual, \mathcal{L}^* , is then given by

$$\mathcal{B} = \begin{pmatrix} 1 & \lambda & \lambda^2 \\ 1 & \operatorname{Re}(\alpha) & \operatorname{Re}(\alpha^2) \\ 0 & \operatorname{Im}(\alpha) & \operatorname{Im}(\alpha^2) \end{pmatrix} \quad \text{and} \quad \mathcal{B}^* = \frac{\operatorname{Im}(\alpha)}{\sqrt{11}} \begin{pmatrix} \lambda^2 - \lambda - 1 & \lambda - 1 & 1 \\ 2\lambda^2 - \lambda & 1 - \lambda & -1 \\ \frac{3\lambda - \lambda^2}{2\operatorname{Im}(\alpha)} & \frac{3(\lambda^2 - 1)}{2\operatorname{Im}(\alpha)} & \frac{1 - 3\lambda}{2\operatorname{Im}(\alpha)} \end{pmatrix}$$

with $\det(\mathcal{B}) = \operatorname{Im}(\alpha)(3\lambda^2 - 2\lambda - 1) = \sqrt{11}$. From the first line of \mathcal{B}^* , one can now extract the Fourier module in our setting from an independent calculation, which gives

$$L^{\otimes} = \vartheta \langle \lambda^2 - \lambda - 1, \lambda - 1, 1 \rangle_{\mathbb{Z}} = \vartheta L,$$

with $\vartheta = (3\lambda^2 - 2\lambda - 1)^{-1}$, in agreement with our general formula (22). The Abelian group L^{\otimes} is also the dynamical spectrum (in additive notation) of our systems; compare Remark 3.1. In fact, Tribonacci and twisted Tribonacci are metrically isomorphic by the Halmos–von Neumann theorem, but have rather different eigenfunctions. Also, they are obviously *not* mutually locally derivable (MLD) from one another; see [6, Sec. 5.2] for background. Moreover, they are not topologically conjugate either, as they can be distinguished via invariants of gauge-theoretic origin [20].

Remark 6.1. The Hausdorff dimension of the fractal boundary of the Tribonacci windows is known; compare [34] as well as [16, Ex. 4.2]. It can be calculated as a similarity dimension, which here is given as the real solution s_H to the equation $|\alpha|^{4s_H} + 2|\alpha|^{3s_H} = 1$. This gives

$$s_H = 2 \frac{\log(b)}{\log(\lambda)} \approx 1.093364,$$

where b is the positive real root of $x^4 - 2x - 1$.

Likewise, for twisted Tribonacci, the Hausdorff dimension of the window boundary is given by [16, Ex. 4.3]

$$s_H = 2 \frac{\log(b)}{\log(\lambda)} \approx 1.791903,$$

where b now is the positive real root of $x^6 - x^5 - x^4 - x^2 + x - 1$, as one derives from the corresponding graph-directed IFS for the boundary; see also [45, Sec. 6.9].

The much larger Hausdorff dimension for the twisted case corresponds to a slower decay of the Fourier transform; see [31, App. B] for an explicit one-dimensional example for which the Fourier transform shows a power-law decay with exponent $1 - d_B$, where d_B is the fractal dimension of the boundary, and [21] for an interesting asymptotic scaling analysis of such

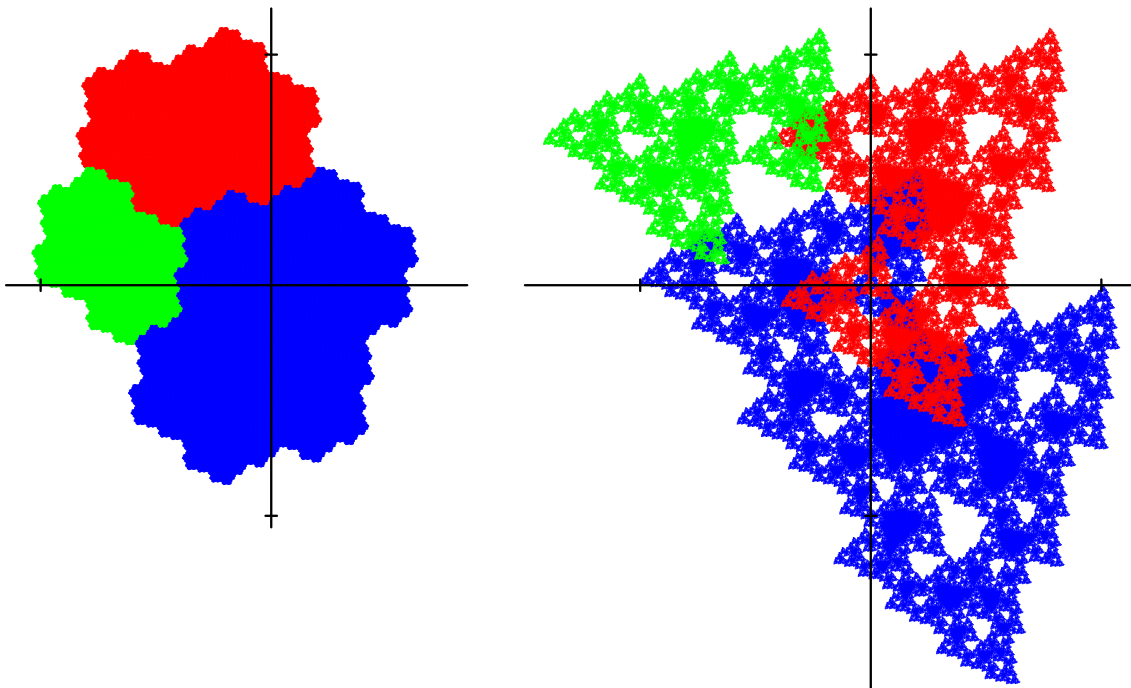


FIGURE 1. Rauzy fractals for the Tribonacci inflation (left panel) and its twisted sibling (right panel), shown at the same scale. They are the windows for the points of type a (blue), b (red) and c (green). The coordinate axes are those emerging from the Minkowski embedding, with ticks indicating unit distances.

coefficients. It would be useful to establish a general result along these lines, which is of recent interest also with respect to a refinement of the notion of complexity [19]. \diamond

If $\sigma_1 : \mathbb{Q}(\lambda) \rightarrow \mathbb{Q}(\alpha)$ is the field isomorphism induced by $\lambda \mapsto \alpha$, one determines the \star -map of $k \in L^\otimes$ as $k \mapsto k^\star := (\operatorname{Re}(\sigma_1(k)), \operatorname{Im}(\sigma_1(k)))^T$. For $k = k_{p,q,r} := \vartheta(p + q\lambda + r\lambda^2)$, this gives

$$k_{p,q,r}^\star = \begin{pmatrix} \frac{1}{44}((-p + 4q + 17r) - (9p - 3q + r)\lambda + (4p - 5q - 2r)\lambda^2) \\ \frac{1}{4\sqrt{11}}((-p + 2q + r) + 3(p + q + r)\lambda - (3q + 2r)\lambda^2) \end{pmatrix},$$

where the integers p, q, r are known as the *Miller indices* of the corresponding Bragg peak in crystallography.

In Figure 2, we compare the peaks of the pure point diffraction measure for the Tribonacci point set and its twisted sibling. The support is the same, but the intensities show characteristic differences. The latter are calculated as

$$I(p, q, r) = \left(\frac{5 + \lambda + 2\lambda^2}{22} \right)^2 |\langle 1 | C(k_{p,q,r}^\star) | v \rangle|^2$$

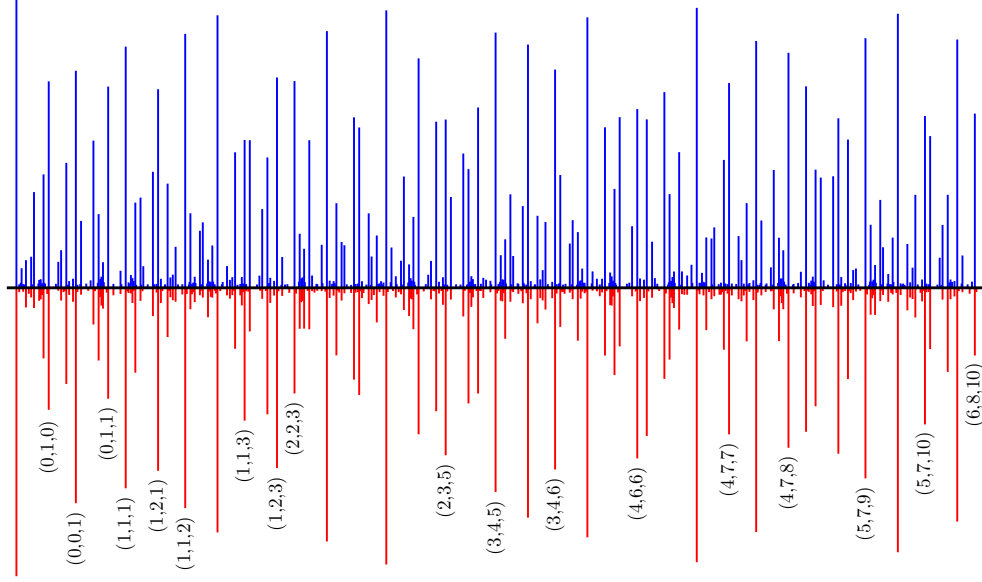


FIGURE 2. Diffraction intensities (Bragg peaks) for the Tribonacci point set (upper part, blue) and for its twisted counterpart (lower part, red). Displayed are the relevant peaks for $k \in L^{\otimes} \cap [0, 10]$, with the intensity represented by the length of the line. The left-most peak is located at the origin and has height $\text{dens}(A)^2$, where $\text{dens}(A) = \frac{1}{22}(5 + \lambda + 2\lambda^2) \approx 0.618420$. Selected peaks are labelled by their Miller index triples.

with the appropriate matrix function C for the two cases. The peaks of the twisted case are often smaller than their untwisted counterparts. Note also that an approximation of the diffraction measure by exponential sums of large patches suffers from slow convergence, in particular for the twisted version, as was previously observed and discussed for the plastic number PV inflation [7]. This reference also contains an illustration of the full Fourier transform of the plastic number Rauzy fractal, which shows similar features as our case at hand.

6.3. The quartic case. Let us briefly consider $\varrho_4 = (01, 02, 03, 0)$ on $\mathcal{A} = \{0, 1, 2, 3\}$, where $\mathbb{Q}(\lambda)$ is a quartic field. Beyond the PF eigenvalue $\lambda \approx 1.927562$, M has one real root μ , with $\mu \approx -0.774804$, and a complex conjugate pair $\alpha, \bar{\alpha}$, with $\alpha \approx -0.076379 + 0.814704i$. For the natural choice of interval lengths, $(\lambda, \lambda^2 - \lambda, \lambda^3 - \lambda^2 - \lambda, 1)$, the Fourier module becomes

$$L^{\otimes} = \vartheta \langle \lambda^3 - \lambda^2 - \lambda - 1, \lambda^2 - \lambda - 1, \lambda - 1, 1 \rangle_{\mathbb{Z}} = \vartheta \mathbb{Z}[\lambda],$$

where

$$\vartheta = (\lambda^3 - 3\lambda^2 - 2\lambda - 1)^{-1} = \frac{1}{563}(10 + 157\lambda - 103\lambda^2 + 16\lambda^3).$$

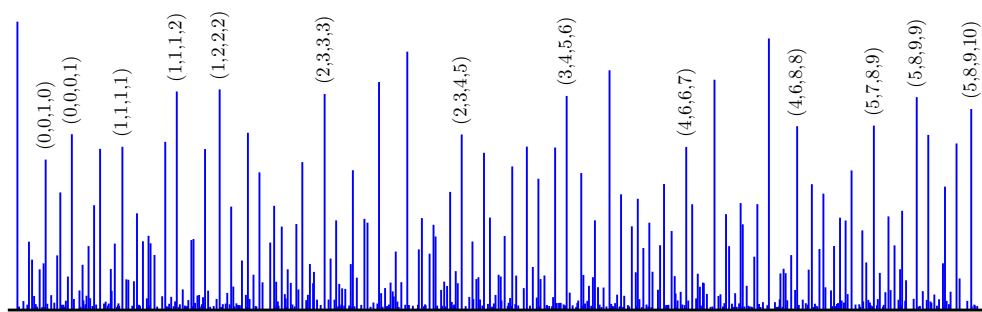


FIGURE 3. Illustration of the pure point diffraction spectrum for the $d = 4$ Pisa inflation, for $k \in L^{\otimes} \cap [0, 10]$. The left-most peak is located at 0 and has height $\text{dens}(\Lambda)^2$, with $\text{dens}(\Lambda) = \frac{1}{563}(86 - \lambda + 15\lambda^2 + 25\lambda^3) \approx 0.566343$. Selected peaks are labelled by their Miller index quadruples.

This follows from (22) and can be verified via the quadratic form $\text{tr}(xy)$, observing $\text{tr}(1) = 4$ and $\text{tr}(\lambda^m) = 2^m - 1$ for $m \in \{1, 2, 3\}$. In analogy to before, we parametrise $k \in L^{\otimes}$ by a quadruple (p, q, r, s) of Miller indices.

The internal Fourier matrix reads

$$\underline{B}(y) = \begin{pmatrix} 1 & 1 & 1 & 1 \\ e(y) & 0 & 0 & 0 \\ 0 & e(y) & 0 & 0 \\ 0 & 0 & e(y) & 0 \end{pmatrix}$$

with $e(y) := \exp(2\pi i(\mu y_1 + \text{Re}(\alpha)y_2 + \text{Im}(\alpha)y_3))$. A calculation analogous to our previous ones leads to the diffraction measure as illustrated in Figure 3. Let us briefly mention that, using the methods from [45, Cor. 4.118 and Prop. 4.122], one can derive an upper bound of 2.327 for the Hausdorff dimension of the window boundaries [46]. It is no problem to twist ϱ_4 , as we did for the Tribonacci case, but we leave further details to the interested reader.

7. TWISTED EXTENSIONS OF FIBONACCI CHAINS WITH MIXED SPECTRUM

Let us close with a simple system with mixed spectrum. It is based on the idea, taken from [4], of a twisted extension of $\varrho_{\mathbb{F}} = (ab, a)$, which is ϱ_2 from Section 6.1, with a *bar swap symmetry*. As such, it works with the extended alphabet $\mathcal{A} = \{a, \bar{a}, b, \bar{b}\}$, where we consider

$$\varrho = (ab, \bar{a}\bar{b}, \bar{a}, a).$$

The natural interval lengths are those of the Fibonacci tiling, so τ for a and \bar{a} , as well as 1 for b and \bar{b} . Also, by identifying a with \bar{a} and b with \bar{b} , one sees that the system possesses the Fibonacci tiling as a topological factor, where the factor map is $2 : 1$ almost everywhere, but not everywhere [20]. Consequently, we have a non-trivial point spectrum, together with a continuous component. The latter, by an application of the renormalisation methods from [5, 32, 33], must be singular continuous.

The substitution matrix of ϱ has spectrum $\{\tau, 1 - \tau, \frac{1}{2}(1 \pm i\sqrt{3})\}$, and a reducible characteristic polynomial. Only the factor with τ as a root is relevant, and one checks that the same embedding as for the Fibonacci tiling can be used. Here, the embedding method produces covering supersets, where the contractive IFS on $(\mathcal{K}\mathbb{R})^4$ reads

$$\begin{aligned} W_a &= \sigma W_a \cup \sigma W_{\bar{b}}, & W_b &= \sigma W_a + \sigma, \\ W_{\bar{a}} &= \sigma W_{\bar{a}} \cup \sigma W_b, & W_{\bar{b}} &= \sigma W_{\bar{a}} + \sigma, \end{aligned}$$

with $\sigma = \tau^*$ as before. The unique solution with compact subsets of \mathbb{R} is

$$(23) \quad \begin{aligned} W_a &= W_{\bar{a}} = [-\sigma^2, -\sigma] = [\tau - 2, \tau - 1] \quad \text{and} \\ W_b &= W_{\bar{b}} = [-1, -\sigma^2] = [-1, \tau - 2], \end{aligned}$$

as can easily be verified by direct computation. Here, we are in the situation that $m_c(y) = 2$ for a.e. $y \in [-1, \tau - 1]$, and uniform distribution is preserved both in the individual windows, by Theorem 5.3, and in the total window.

Note that the point sets Λ_a^* and $\Lambda_{\bar{a}}^*$ are disjoint, but have the same closure, and analogously for Λ_b^* and $\Lambda_{\bar{b}}^*$. The right-hand sides of the window equations are measure-disjoint by Lemma 3.4, which means that the cocycle approach can be applied, with the window covering degree being $m_c = 2$. Since uniform distribution is satisfied here by Theorem 5.3, the FB coefficients from (19) can be calculated by means of (21). For weights $h_\alpha \in \mathbb{C}$ with $\alpha \in \{a, \bar{a}, b, \bar{b}\}$, the pure point part of the diffraction reads

$$(\hat{\gamma})_{\text{pp}} = \sum_{k \in L^\circledast} \left| \sum_{\alpha} h_\alpha A_\alpha(k) \right|^2 \delta_k,$$

with the additional part of the diffraction measure being singular continuous.

As was noticed by Gähler [20], one can employ a partial return word coding to arrive at another inflation which defines a tiling system that is MLD with the above. Concretely, consider the alphabet $\{A, B, C, D\}$ and the inflation $\varrho' = (AB, D, CA, C)$. Here, A and B correspond to a and b , while C replaces $\bar{a}\bar{b}$ and D replaces each \bar{a} that is not followed by a \bar{b} . This gives the substitution matrix

$$\begin{pmatrix} 1 & 0 & 1 & 0 \\ 1 & 0 & 0 & 0 \\ 0 & 0 & 1 & 1 \\ 0 & 1 & 0 & 0 \end{pmatrix}$$

with the same eigenvalues as above. The natural interval lengths are $(\tau, 1, \tau + 1, \tau)$, in agreement with the local derivation rule just stated.

The resulting window equations read

$$W_A = \sigma W_A \cup (\sigma W_C + \sigma^2), \quad W_B = \sigma W_A + \sigma, \quad W_C = \sigma W_C \cup \sigma W_D, \quad W_D = \sigma W_B,$$

which constitute a contractive IFS on $(\mathcal{K}\mathbb{R})^4$ with unique solution

$$W_A = [\tau - 2, \tau - 1], \quad W_B = [-1, \tau - 2], \quad W_C = [\tau - 2, 2\tau - 3], \quad W_D = [2\tau - 3, \tau - 1].$$

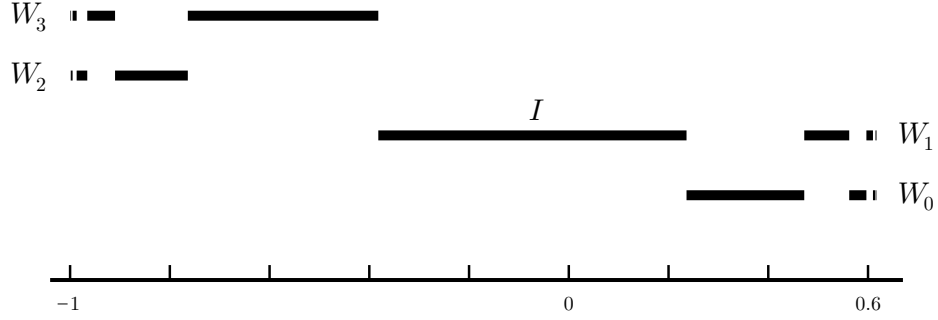


FIGURE 4. Illustration of the four windows for the primitive inflation rule $\tilde{\varrho} = (12, 13, 1, 0)$. Note that $W_0 \cup W_1 = [-\sigma^2, -\sigma]$ and $W_2 \cup W_3 = [-1, -\sigma^2]$, while $I = [-\sigma^2, -\sigma^3]$.

The total window is $[-1, \tau - 1]$ as in the twisted Fibonacci example, but the window function $\mathfrak{m}_c(x)$ now is a step function as induced by

$$(24) \quad \begin{array}{c} \text{---} W_A \text{---} \\ \tau-2 \qquad \qquad \tau-1 \\ \text{---} W_B \text{---} W_C \text{---} W_D \text{---} \\ -1 \qquad \tau-2 \qquad 2\tau-3 \qquad \tau-1 \end{array}$$

As was further analysed by Gähler [20], there is also a maximal topological pure point factor such that the factor map is 2:1 everywhere. Using the alphabet $\{0, 1, 2, 3\}$, this maximal pure point factor is given by the inflation rule

$$\tilde{\varrho} = (12, 13, 1, 0),$$

where 0 and 1 stand for intervals of length τ , while those of type 2 and 3 have unit length. The factor map can most easily be given as a block map, where words of length 2 at position n are mapped to an element of the new alphabet at the same position, namely

$$(25) \quad aa, \bar{a}\bar{a} \mapsto 0, \quad ab, \bar{a}\bar{b}, a\bar{a}, \bar{a}a \mapsto 1, \quad ba, \bar{b}\bar{a} \mapsto 2, \quad b\bar{a}, \bar{b}a \mapsto 3,$$

and correspondingly for the tilings, where the resulting mapping is called a *local derivation rule*; see [6, Sec. 5.2] for details.

Conversely, one proceeds in two steps. First, any given sequence from the (symbolic) hull of $\tilde{\varrho}$ is mapped to a sequence in $\{a, b\}^{\mathbb{Z}}$ by $0, 1 \mapsto a$ and $2, 3 \mapsto b$. In the second step, choose one position and decide whether to place a bar on the letter or not. Then, the bar status of the two neighbouring symbols is uniquely determined from the original block map (25), read backwards. Inductively, this fixes the entire sequence. Since the only choice was the initial bar, this shows that the block map (25) is globally 2:1. Once again, this block map transfers to a local derivation rule for the corresponding tilings.

The new inflation rule $\tilde{\varrho}$ leads to a regular model set, with window equations

$$W_0 = \sigma W_3, \quad W_1 = \sigma W_0 \cup \sigma W_1 \cup \sigma W_2, \quad W_2 = \sigma W_0 + \sigma, \quad W_3 = \sigma W_1 + \sigma.$$

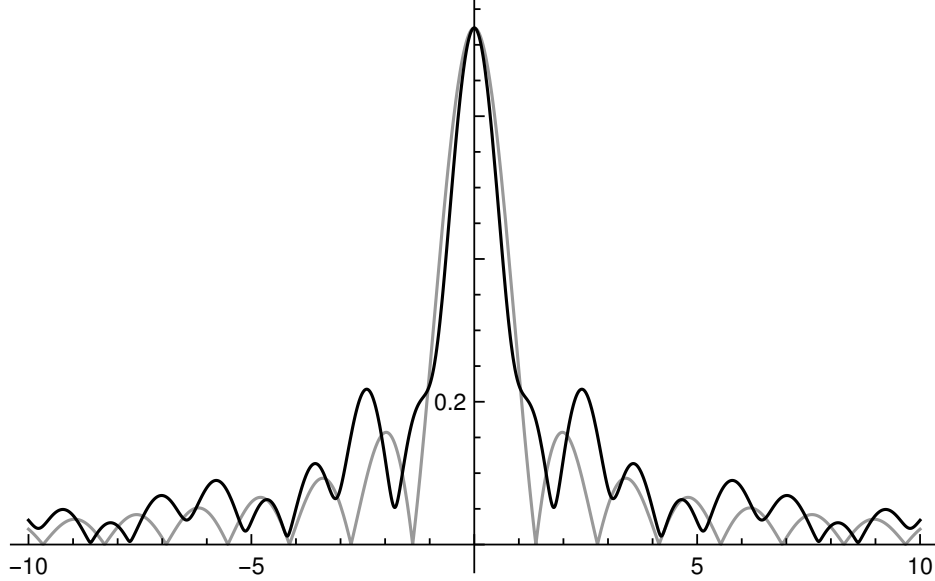


FIGURE 5. Illustration of $|\widetilde{1_{W_1}}(y)|$ (black curve) in comparison with the modulus of the Fourier transform of an interval of length $\frac{\tau+2}{5}$ (grey curve), which is the value at 0 for both functions.

Due to the factor map, we immediately know that $W_0 \cup W_1 = W_a$ and $W_2 \cup W_3 = W_b$ with W_a and W_b from (23). The unique solution can be determined by first observing that each W_i with $i \neq 1$ can be expressed in terms of W_1 . This gives a rescaling equation for W_1 alone, namely

$$W_1 = \sigma W_1 \cup (\sigma^3 W_1 + \sigma^3) \cup (\sigma^4 W_1 + \sigma^4 + \sigma^2) = I \cup g(W_1),$$

where $I = (W_2 \cup W_3) - \sigma = [-\sigma^2, -\sigma^3]$ and $g(x) = \sigma^4 x + \sigma^4 + \sigma^2$.

This leads to $W_1 = I \cup g(I) \cup g(g(I)) \cup \dots$ which results in the formula

$$(26) \quad W_1 = \bigcup_{n \geq 0} (\sigma^{4n} [-\sigma^2, -\sigma^3] + \sigma(\sigma^{4n} - 1)),$$

while the other windows follow from here via affine mappings. All four windows are illustrated in Figure 4, each comprising countably many disjoint intervals.

The explicit expression for W_1 in (26) leads to the (inverse) Fourier transform of its characteristic function in the form

$$(27) \quad f_1(y) = \widetilde{1_{W_1}}(y) = - \sum_{n=0}^{\infty} \sigma^{4n+1} e^{-\pi i(2\sigma + 2\sigma^{4n} + \sigma^{4n+1})y} \operatorname{sinc}(\pi \sigma^{4n+1} y)$$

with $f_1(0) = \tau/\sqrt{5} = \frac{\tau+2}{5}$, which is the total length of the window W_1 ; see Figure 5 for a comparison of $|f_1|$ with the function $|\frac{\tau+2}{5} \operatorname{sinc}(\frac{\tau+2}{5} \pi y)|$.

For the cocycle approach, we first note that the internal Fourier matrix reads

$$\underline{B}(y) = \begin{pmatrix} 0 & 0 & 0 & 1 \\ 1 & 1 & 1 & 0 \\ e^{2\pi i \sigma y} & 0 & 0 & 0 \\ 0 & e^{2\pi i \sigma y} & 0 & 0 \end{pmatrix}$$

with $\underline{B}(0) = M$ as usual. The frequency-normalised right PF eigenvector is

$$|v\rangle = \frac{1}{5}(-1 - 3\sigma, 1 - 2\sigma, 3 + 4\sigma, 2 + \sigma)^T \approx (0.171, 0.447, 0.106, 0.276)^T,$$

where one has $\text{vol}(W_i) = \tau v_i$ for the total window lengths. With $C(y) = \lim_{n \rightarrow \infty} |\sigma|^n \underline{B}^{(n)}(y)$, one gets $f_1(y) = \tau \langle 0, 1, 0, 0 | C(y) | v \rangle$, where the convergence of the underlying matrix product is exponentially fast. Here, one can then study the rate of convergence in comparison to the alternative formula in (27).

8. OUTLOOK

It is possible to extend our approach to inflation tilings in higher dimensions, if the inflation multiplier is a PV unit. In fact, this is needed when dealing with direct product variations (DPV) as considered in [17, 18, 2].

An extension to the non-unit case is also possible, but requires a larger machinery from algebraic number theory, as developed in [45] for the treatment of the Pisot substitution conjecture in the non-unit case.

Finally, also S -adic type inflations can be covered, provided that the participating inflation rules are compatible in the sense that they share the same substitution matrix.

ACKNOWLEDGEMENTS

It is a pleasure to thank N.P. Frank, F. Gähler, N. Mañibo, B. Sing and N. Strungaru for helpful discussions. Our work was supported by the German Research Foundation (DFG), within the CRC 1283 at Bielefeld University, and by EPSRC through grant EP/S010335/1.

REFERENCES

- [1] Akiyama S, Barge M, Berthé V, Lee J-Y and Siegel A, On the Pisot substitution conjecture, in *Mathematics of Aperiodic Order*, eds. Kellendonk J, Lenz D and Savinien J, Birkhäuser, Basel (2015), pp. 33–72.
- [2] Baake M, Frank N P and Grimm U, Three variations on a theme by Fibonacci, in preparation.
- [3] Baake M, Frank N P, Grimm U and Robinson E A, Geometric properties of a binary non-Pisot inflation and absence of absolutely continuous diffraction, *Studia Math.* **247** (2019) 109–154; [arXiv:1706.03976](#).
- [4] Baake M and Gähler F, Pair correlations of aperiodic inflation rules via renormalisation: Some interesting examples, *Topology & Appl.* **205** (2016) 4–27; [arXiv:1511.00885](#).
- [5] Baake M, Gähler F and Mañibo N, Renormalisation of pair correlation measures for primitive inflation rules and absence of absolutely continuous diffraction, *Commun. Math. Phys.*, in press; [arXiv:1805.09650](#).

- [6] Baake M and Grimm U, *Aperiodic Order. Vol. 1: A Mathematical Invitation*, Cambridge University Press, Cambridge (2013).
- [7] Baake M and Grimm U, Diffraction of a model set with complex windows, *J. Phys.: Conf. Ser.*, in press; [arXiv:1904.08285](#).
- [8] Baake M and Lenz D, Dynamical systems on translation bounded measures: Pure point dynamical and diffraction spectra, *Ergod. Th. & Dynam. Syst.* **24** (2004) 1867–1893; [arXiv:math.DS/0302061](#).
- [9] Baake M and Lenz D, Spectral notions of aperiodic order, *Discr. Cont. Dynam. Syst. S* **10** (2018) 161–190; [arXiv:1601.06629](#).
- [10] Baake M and Moody R V, Self-similar measures for quasicrystals, in *Directions in Mathematical Quasicrystals*, eds. Baake M and Moody R V, CRM Monograph Series, vol. 13, AMS, Providence, RI (2000), pp. 1–42; [arXiv:math.MG/0008063](#).
- [11] Baake M and Sing B, Kolakoski-(3, 1) is a (deformed) model set, *Can. Math. Bull.* **47** (2004) 168–190; [arXiv:math.MG/0206098](#).
- [12] Barreira L and Pesin Y, *Nonuniform Hyperbolicity: Dynamics of Systems with Nonzero Lyapunov Exponents*, Cambridge University Press, Cambridge (2007).
- [13] Brauer A, On algebraic equations with all but one root in the interior of the unit circle, *Math. Nachr.* **4** (1950/51) 250–257.
- [14] Clark A and Sadun L, When size matters: Subshifts and their related tiling spaces, *Ergod. Th. & Dynam. Syst.* **23** (2003) 1043–1057; [arXiv:math.DS/0201152](#).
- [15] Clark A and Sadun L, When shape matters: Deformation of tiling spaces, *Ergod. Th. & Dynam. Syst.* **26** (2006) 69–86; [arXiv:math.DS/0306214](#).
- [16] Feng D-J, Furukado M, Ito S and Wu J, Pisot substitutions and the Hausdorff dimension of boundaries of atomic surfaces, *Tsukuba J. Math.* **26** (2006) 195–223.
- [17] Frank N P, A primer of substitution tilings of the Euclidean plane, *Expo. Math.* **26** (2008) 295–326; [arXiv:0705.1142](#).
- [18] Frank N P and Robinson E A, Generalized β -expansions, substitution tilings, and local finiteness, *Trans. Amer. Math. Soc.* **360** (2008) 1163–1177; [arXiv:math.DS/0506098](#).
- [19] Fuhrmann G and Gröger M, Constant length substitutions, iterated function systems and amorphous complexity, *Preprint* [arXiv:1812.10789](#).
- [20] Gähler F, private communication (2019).
- [21] Godrèche C and Luck J M, Multifractal analysis in reciprocal space and the nature of the Fourier transform of self-similar structures, *J. Phys. A: Math. Gen.* **23** (1990) 3769–3797.
- [22] Horn R A and Johnson C R, *Matrix Analysis*, 2nd ed., Cambridge University Press, Cambridge (2013).
- [23] Householder A S, *The Theory of Matrices in Numerical Analysis*, reprint, Dover, New York (1975).
- [24] Huck C and Richard C, On pattern entropy of weak model sets, *Discr. Comput. Geom.* **54** (2015) 714–757; [arXiv:1412.6307](#).
- [25] Ito S and Rao H, Atomic surfaces, tilings and coincidence I. Irreducible case, *Israel J. Math.* **153** (2006) 129–156.
- [26] Johnson C R and Nylén P, Monotonicity properties of norms, *Lin. Alg. Appl.* **148** (1991) 43–58.
- [27] Lagarias J C and Pleasants P A B, Repetitive Delone sets and quasicrystals, *Ergod. Th. & Dynam. Syst.* **23** (2003) 831–867; [arXiv:math.DS/9909033](#).

- [28] Lagarias J C and Wang Y, Substitution Delone sets, *Discr. Comput. Geom.* **29** (2003) 175–209; [arXiv:math.MG/0110222](https://arxiv.org/abs/math/0110222).
- [29] Lee J-Y, Moody R V and Solomyak B, Pure point dynamical and diffraction spectra, *Ann. H. Poincaré* **2** (2002) 1003–1018; [arXiv:0910.4809](https://arxiv.org/abs/0910.4809).
- [30] Lenz D, Continuity of eigenfunctions of uniquely ergodic dynamical systems and intensity of Bragg peaks, *Commun. Math. Phys.* **287** (2009) 225–258; [arXiv:math-ph/0608026](https://arxiv.org/abs/math-ph/0608026).
- [31] Luck J M, Godrèche C, Janner A and Janssen T, The nature of the atomic surfaces of quasiperiodic self-similar structures, *J. Phys. A: Math. Gen.* **26** (1993) 1951–1999.
- [32] Mañibo C N, *Lyapunov Exponents in the Spectral Theory of Primitive Inflation Systems*, PhD thesis, Bielefeld University (2019); available at <https://pub.uni-bielefeld.de/record/2935972>.
- [33] Mañibo C N, private communication (2019).
- [34] Messaoudi A, Frontière du fractals de Rauzy et système de numération complexe, *Acta Arithm.* **95** (2000) 195–224.
- [35] Moody R V, Model sets: A survey, in *From Quasicrystals to More Complex Systems*, eds. Axel F, Dénoyer F and Gazeau J P, EDP Sciences, Les Ulis, and Springer, Berlin (2000), pp. 145–166; [arXiv:math.MG/0002020](https://arxiv.org/abs/math/0002020).
- [36] Neukirch J, *Algebraic Number Theory*, Springer, Berlin (1999).
- [37] Pleasants P A B, Designer quasicrystals: Cut and project sets with pre-assigned properties, in *Directions in Mathematical Quasicrystals*, eds. Baake M and Moody R V, CRM Monograph Series, vol. 13, AMS, Providence, RI (2000), pp. 95–141.
- [38] Pohl A D, Symbolic dynamics, automorphic functions, and Selberg zeta functions with unitary representations, *Contemp. Math.* **669** (2016) 205–236; [arXiv:1503.00525](https://arxiv.org/abs/1503.00525).
- [39] Pytheas Fogg N, *Substitutions in Dynamics, Arithmetics and Combinatorics*, LNM 1794, Springer, Berlin (2002).
- [40] Queffélec M, *Substitution Dynamical Systems — Spectral Analysis*, 2nd ed., LNM 1294, Springer, Berlin (2010).
- [41] Rauzy G, Nombres algébriques et substitutions, *Bull. Soc. Math. France* **110** (1982) 147–178.
- [42] Reed M and Simon B, *Methods of Modern Mathematical Physics. I. Functional Analysis*, 2nd ed., Academic Press, San Diego, CA (1980).
- [43] Schlottmann M, Cut-and-project sets in locally compact Abelian groups, in *Quasicrystals and Discrete Geometry*, ed. Patera J, Fields Institute Monographs, vol. 10, AMS, Providence, RI (1998), pp. 247–264.
- [44] Siegel A and Thuswaldner J M, *Topological Properties of Rauzy Fractals*, Mém. Soc. Math. France 118, Société Mathématiques de France, Paris (2009).
- [45] Sing B, *Pisot Substitutions and Beyond*, PhD thesis, Bielefeld University (2007); available at <https://pub.uni-bielefeld.de/record/2302336>.
- [46] Sing B, private communication (2019).
- [47] Sloane N J A, The On-Line Encyclopedia of Integer Sequences; available at <http://oeis.org/>.
- [48] Solomyak B, Dynamics of self-similar tilings, *Ergod. Th. & Dynam. Syst.* **17** (1997) 695–738; Erratum, *Ergod. Th. & Dynam. Syst.* **19** (1999) 1685.
- [49] Strungaru N, Almost periodic measures and long-range order in Meyer sets, *Discr. Comput. Geom.* **33** (2005) 483–505.

- [50] Strungaru N, Almost periodic pure point measures, in *Aperiodic Order. Vol. 2: Crystallography and Almost Periodicity*, eds. Baake M and Grimm U, Cambridge University Press, Cambridge (2017), pp. 271–342; [arXiv:1501.00945](https://arxiv.org/abs/1501.00945).

FAKULTÄT FÜR MATHEMATIK, UNIVERSITÄT BIELEFELD,
POSTFACH 100131, 33501 BIELEFELD, GERMANY
E-mail address: mbaake@math.uni-bielefeld.de

SCHOOL OF MATHEMATICS AND STATISTICS, THE OPEN UNIVERSITY,
WALTON HALL, MILTON KEYNES MK7 6AA, UK
E-mail address: uwe.grimm@open.ac.uk